Review

Development and Evolution of DNA-Dependent Protein Kinase Inhibitors toward Cancer Therapy

Yoshihisa Matsumoto

Laboratory for Zero-Carbon Energy, Institute of Innovative Research, Tokyo Institute of Technology, Tokyo 152-8550, Japan; yoshim@zc.iir.titech.ac.jp; Tel.: +81-3-5734-2273

Abstract: DNA double-strand break (DSB) is considered the most deleterious type of DNA damage, which is generated by ionizing radiation (IR) and a subset of anticancer drugs. DNA-dependent protein kinase (DNA-PK), which is composed of a DNA-PK catalytic subunit (DNA-PKcs) and Ku80-Ku70 heterodimer, acts as the molecular sensor for DSB and plays a pivotal role in DSB repair through non-homologous end joining (NHEJ). Cells deficient for DNA-PKcs show hypersensitivity to IR and several DNA-damaging agents. Cellular sensitivity to IR and DNA-damaging agents can be augmented by the inhibition of DNA-PK. A number of small molecules that inhibit DNA-PK have been developed. Here, the development and evolution of inhibitors targeting DNA-PK for cancer therapy is reviewed. Significant parts of the inhibitors were developed based on the structural similarity of DNA-PK to phosphatidylinositol 3-kinases (PI3Ks) and PI3K-related kinases (PIKKs), including Ataxia-telangiectasia mutated (ATM). Some of DNA-PK inhibitors, e.g., NU7026 and NU7441, have been used extensively in the studies for cellular function of DNA-PK. Recently developed inhibitors, e.g., M3814 and AZD7648, are in clinical trials and on the way to be utilized in cancer therapy in combination with radiotherapy and chemotherapy.

Keywords: DNA double-strand break (DSB); non-homologous end joining (NHEJ); DNA-dependent protein kinase (DNA-PK); phosphatidylinositol 3-kinase; inhibitor; radiosensitization; chemosensitization

1. Introduction

Ionizing radiation (IR) is thought to exert a variety of biological effects through the induction of damages on DNA. One Gy of X-ray or γ-ray is estimated to induce approximately 500 thymine glycols, 150 DNA-protein crosslinks, 1000 single-strand breaks, and 40 double-strand breaks (DSBs) [1]. DSB is considered the most deleterious among the various types of DNA damage.

In eukaryotes, DSB is repaired mainly through homologous recombination (HR) and non-homologous end joining (NHEJ) [2]. There are two other pathways, i.e., alternative end joining (A-EJ) and single-strand annealing (SSA) [2]. A-EJ is also termed microhomology-mediated end joining (MMEJ) or DNA polymerase theta-mediated end joining (TMEJ). These four pathways are distinguished by their usage of sequence homology (Figure 1). HR reconstitutes the DNA sequence around DSB using a homologous or identical sequence as the template, which is usually longer than 100 base pairs (bp). On the other hand, NHEJ utilizes little or no sequence homology, i.e., 0–4 bp. A-EJ and SSA utilize sequence homology of 2–20 bp and more than 50 bp, respectively. HR, A-EJ and SSA are preceded by the end resection, which creates single-stranded DNA with 3′-overhang. The end resection proceeds in two stages, i.e., initial short-range resection ($\approx$100 nucleotides (nt)) followed by long-range resection (several hundred or thousand nt). While A-EJ requires only short-range resection, HR and SSA require long-range resection.
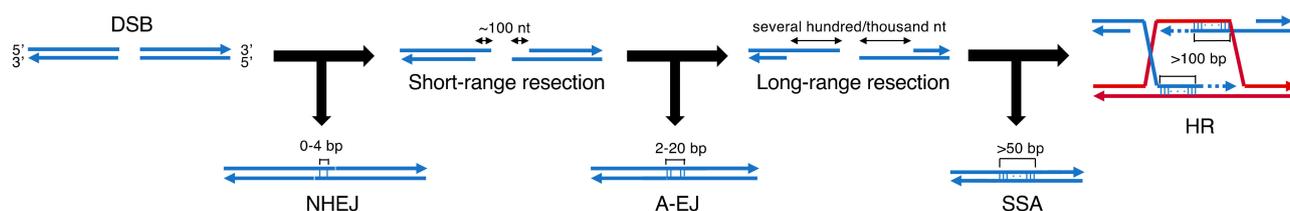
Figure 1. DNA double-strand break pathways. DSB: DNA double-strand break, NHEJ: non-homologous end joining, A-EJ: alternative end joining, SSA: single-strand annealing, HR: homologous recombination.

In NHEJ, the DNA ends that are not compatible for ligation undergo end processing, which results in the deletion or insertion of nucleotides at the junction. In addition, joining of the ends in close vicinity may sometimes lead to ligation of incorrect pairs of DNA ends, resulting in chromosomal aberrations such as deletions, inversions, and translocations. Thus, NHEJ is considered more error-prone than HR. However, HR in vertebrates has a requirement for the sister chromatid and is restricted to late S and G2 phases. (Note: a very recent study demonstrated that DSBs at the centromere are repaired through HR even in the G1 phase [3].) The majority of cells are in G1 and G0 phases, in which cells rely on NHEJ to repair DSBs. In human cells, NHEJ accounts for approximately 80% of DSB repair even in the G2 phase [2]. Moreover, in most cases, the deletion or insertion of a small number of nucleotides can be tolerated, because only a small portion of the genome encodes proteins. A-EJ and SSA are thought to be more error-prone than NHEJ, because they are apt to occur between repetitive sequences, resulting in the loss of the sequence in between.

NHEJ is also implicated in the process of V(D)J recombination in vertebrate immune system [2]. Enormous diversity of immunoglobulins and T cell receptors are generated through the recombination of V (variable), D (diversity), and J (joining) segments, each of which can be selected from a number of segments. Recombination activating gene 1 and 2 (RAG1 and RAG2) induce a cleavage between the selected segments and the flanking recombination signal sequences. Then, the segments are joined through NHEJ. Thus, NHEJ is thought to be of prominent importance especially in vertebrates such as humans.

2. DNA-PK and Its Role NHEJ

DNA-dependent protein kinase (DNA-PK) is composed of a DNA-PK catalytic subunit (DNA-PKcs) and Ku heterodimer (hereafter denoted Ku), which consists of Ku80 (also termed Ku86) and Ku70 [4,5]. DNA-PK binds to and is activated by the end of a double-stranded DNA (dsDNA). Thus, DNA-PK acts as the sensor for the end of dsDNA, which appears when a DSB is generated.

DNA-PKcs is a huge protein consisting of 4128 amino acids (Figure 2A) [6]. DNA-PKcs is structurally related to Ataxia-telangiectasia mutated (ATM) and ATM- and Rad3-related (ATR) kinases, which are also implicated in DNA repair and DNA damage response [6–9]. ATM is recruited to DSB by the MRN complex consisting of Mre11, Rad50 and Nbs1, the last of which is responsible for Nijmegen breakage syndrome [10,11]. ATR is recruited to ssDNA through interaction with ATR-interacting protein (ATRIP) and Replication Protein A (RPA) [12]. These kinases show structural similarity to phosphatidylinositol 3-kinases (PI3Ks) and assemble the PIKK family. There are three additional PIKK members in humans, i.e., mammalian Target of rapamycin (mTOR, also termed FKBP12-rapamycin-associated protein, FRAP, and Rapamycin and FKBP12-target, RAFT) [13,14], Suppressor of morphological defects on genitalia-1 (SMG-1) [15,16], and Transformation/transcription domain-associated protein (TRRAP) [17]. Interestingly, TRRAP lacks kinase catalytic activity [17]. In addition to the kinase domain, these proteins share the FAT (FRAP, ATM and TRRAP), PRD (PIKK-regulatory domain) and FATC (FAT C-terminal) domains (Figure 2A). The primary function of mTOR is the regulation of cell growth and survival [13,14]. SMG-1 is essential for nonsense-mediated mRNA decay (NMD) [15,16]. PI3Ks mediates the signals from G-protein coupled receptors and receptor tyrosine kinases through the activation

of AKT protein kinase (also known as protein kinase B, PKB) and mTOR [18–20]. This signaling pathway is called the PI3K/AKT/mTOR pathway. There are lines of evidence implicating these molecules in DNA damage response, although less directly than DNA-PKcs, ATM, and ATR [18–20]. SMG-1 was shown to activate the G1/S checkpoint through p53 upregulation and Cdc25A downregulation [21,22]. Recent studies showed that the human papilloma virus E6 protein and DNMT1 enhance radiosensitivity via the down-regulation of SMG-1 [23,24]. The PI3K/AKT/mTOR pathway is upregulated in response to radiation and promotes cell survival [25]. AKT inhibits apoptosis through the down-regulation of proapoptotic proteins, such as B cell lymphoma 2 associated agonist of cell death (BAD) [26,27] and upregulation of antiapoptotic proteins, such as human homolog of murine double minute 2 (HDM2), which promotes the degradation of p53 [28]. It is also reported that AKT augments NHEJ and HR [29,30]. Moreover, DNA-PK is shown to activate AKT in response to DNA damage directly or indirectly via Sty1/Spc1-interacting protein 1 (Sin1) [31,32]. The upregulation of the PI3K/AKT/mTOR pathway is frequently found in various types of cancer and is associated with resistance to radiotherapy and chemotherapy [18–20]. Thus, mTOR and PI3Ks are considered promising targets for radiosensitization and chemosensitization.

Ku80 and Ku70 consist of 732 and 609 amino acids, respectively (Figure 2B) [33,34]. Ku was initially identified as the antigen against autoantibody in a patient with an autoimmune disease, scleroderma-polymyositis overlap syndrome. Ku binds to the end of dsDNA without any particular preference in the nucleotide sequence [35]. DNA-PKcs is recruited to the end of dsDNA via interaction with the C-terminal region of Ku80 [36].

X-ray crystallography showed that Ku forms a ring-shaped structure that can encircle DNA, accounting for how Ku binds selectively to DNA ends [37]. Recent cryoelectron microscopy (cryo-EM) studies revealed a structure of DNA-PKcs complexed with Ku and DNA [38] (Figure 2C). DNA-PKcs is folded into a ring and a head. The ring includes the HEAT repeats and the interface with Ku, while the head includes FAT, kinase, PRD, and FAT-C domains [38]. DNA is inserted into the rings of Ku and DNA-PKcs [38]. The structural differences between inactive and active states of DNA-PKcs are also revealed. Most notably, PRD is closed in the inactive state and is assumed to clash with the substrate polypeptide. However, PRD becomes open in the active state, allowing the entry of a substrate polypeptide. Another cryo-EM study revealed the structure of DNA-PKcs in a complex with adenosine-5′-(γ-thio)-triphosphate (ATPγS), which is a non-hydrolyzable ATP analog [39] (Figure 2D). The adenine group is inserted into a hydrophobic pocket surrounded by Tyr3791, Trp3805 and Leu3806 [39]. Three phosphate groups and Mg^{2+} ions come in contact with Asn3926, Asn3927, Asp3941, Ser3731 and Lys3753 [39]. These multiple interactions are thought to stabilize the interaction between DNA-PKcs and ATP. While Lys3753, Tyr3791, Trp3805, Asn3927 and Asp3941 are fully conserved among PIKKs, Ser3731, Leu3806 and Asn3926 are divergent. The structures of DNA-PKcs with inhibitors were also elucidated (see below).

Ku and DNA-PKcs have been shown to be essential for NHEJ (Figure 2E and for details, refer to another review [40]). Initially, Ku80 was shown to correspond to X-ray repair cross-complementing group (XRCC) 5, which is deficient in a series of rodent cell lines exhibiting hypersensitivity to IR and defective V(D)J recombination [41,42]. Subsequently, DNA-PKcs was shown to correspond to XRCC7 and to be the responsible gene for murine severe combined immunodeficiency (*scid*) mutation [43–45]. Thereafter, a number of cells and animals deficient for DNA-PKcs, Ku80 or Ku70 were found or generated through gene targeting or genome editing [40]. In addition, six human individuals that harbor homozygous or compound heterozygous mutations in DNA-PKcs have been identified [40].

NHEJ proceeds in three stages (Figure 2E). In the recognition stage, Ku first binds to the end of DNA and then recruits DNA-PKcs. Paralog of XRCC4 and XLF (PAXX) stabilizes the binding of Ku to DNA and facilitates the subsequent assembly of the NHEJ factors [45–48]. When DNA ends are not compatible, they undergo the processing stage (for details, refer to review [2]). Artemis, in a complex with DNA-PKcs, exerts endonuclease

activity on hairpin and overhang structures and 5′ to 3′ exonuclease activity on single-stranded DNA [49,50]. DNA polymerase μ (Polμ) and DNA polymerase λ (Polλ) fill in the gaps in DSBs. Polynucleotide kinase phosphatase (PNKP) adds a phosphate group at the 5′-end if absent and removes the phosphate group present at the 3′-end. Aprataxin (APTX) removes adenosinemonophosphate (AMP) from the abortive intermediates of ligation. Tyrosyl-DNA phosphodiesterase 1 (TDP1) and TDP2 remove the covalently bound proteins and phosphoglycolate groups from 3′-ends. In the ligation stage, DNA ligase IV (LIG4), which is associated with XRCC4, joins two DNA ends together [51–53]. XRCC4-like factor (XLF, also known as Cernunnos) forms filaments with XRCC4, which are suggested to align or bridge two DNA ends [54–56].

The kinase activity of DNA-PKcs is required for NHEJ because the catalytically inactive (kinase-dead) form of DNA-PKcs cannot rescue the radiosensitivity and V(D)J recombination defects of DNA-PKcs-deficient cells [57,58]. Although the precise roles of protein phosphorylation by DNA-PKcs remain elusive, DNA-PKcs is shown to phosphorylate NHEJ factors and other potentially NHEJ-related proteins (Table 1). The significance of phosphorylation of each substrate protein has been discussed elsewhere [59].

Table 1. DNA-PK substrates and their functions.

Substrates	Function	Substrates	Function
[DNA Repair and Damage Signaling]		**[Transcription]**	
(NHEJ)		RNA polymerase II	Transcription (general)
DNA-dependent protein kinase catalytic subunit (DNA-PKcs)	DNA-PK complex	TATA box-binding protein (TBP)	
Ku autoantigen 80kDa subunit (Ku80)		p53	Transcription (specific)
Ku autoantigen 70 kDa subunit (Ku70)		Specificity protein 1 (Sp1)	
		c-Jun	
		c-Fos	
DNA ligase IV (LIG4)	Ligation complex	c-Myc	
X-ray repair cross-complementing group 4 (XRCC4)		Octamer-binding factor 1 (Oct-1)	
XRCC4-like factor (XLF)		Serum response factor (SRF)	
Artemis	Nuclease	**[RNA metabolism]**	
Polynucleotide kinase phosphatase (PNKP)	Kinase, phosphatase	Nuclear DNA helicase II (NDHII)	Transcription and RNA processing
Werner syndrome protein (WRN)	Helicase, nuclease	Heterogeneous nuclear ribonucleoprotein A1 (hnRNP-A1)	RNA splicing
(Other DNA repair and damage signaling pathways)			
Ataxia telangiectasia mutated (ATM)	Protein kinase; HR and cell cycle checkpoint	Heterogeneous nuclear ribonucleoprotein U (hnRNP-U)	
Replication protein A 2 (RPA2)	Single-stranded DNA binding; HR and DNA replication	Fused in sarcoma (FUS)	RNA binding
Poly(ADP-ribose) polymerase 1 (PARP1)	Single-strand break repair	**[Signaling]**	
Excision repair cross complementing 1 (ERCC1)	Nuclease component; nucleotide excision repair	Akt1	Protein kinase
		Akt2	Protein kinase

Table 1. *Cont.*

Substrates	Function	Substrates	Function
[DNA Repair and Damage Signaling]		**[Transcription]**	
[DNA replication]		Sty1/Spc1-interacting protein 1 (Sin1)	Protein kinase regulator
DNA ligase I (LIG1)	Ligation		
Minichromosome maintenance 3 (MCM3)	Initiation of replication	**[Organelle, cytoskeleton]**	
[Nucleosome and chromatin structure]		Golgi phosphoprotein 3 (GOLPH3)	Linking Golgi membrane to cytoskeleton
Histone H2AX	Core histone component; recruitment of DSB repair proteins	Vimentin	Intermediate filament
Histone H1	Linker histone	Tau	Microtubule regulation
High mobility group 1 (HMG1)	Maintenance and regulation of chromatin structure	**[Protein maintenance]**	
High mobility group 2 (HMG2)		Heat shock protein 90 alpha (HSP90a)	Protein chaperone
C1D		Valosin-containing protein (VCP)	AAA+ ATPase
Topoisomerase I	Regulation of topological status of DNA	**[Metabolism]**	
Topoisomerase II		Fumarate hydratase (FH)	Production of L-malate from fumarate; regulation of NHEJ
Nuclear orphan receptor 4A2 (NR4A2)	Chromatin regulation; regulation of NHEJ		
Pituitary tumor-transforming gene (PTTG)	Regulation of chromosome segregation		

A number of small molecules that inhibit DNA-PK have been developed to date. These compounds have been powerful tools to delineate the function of DNA-PK. Furthermore, they are promising agents in cancer therapy, sensitizing cancer cells to radiotherapy and chemotherapy. Hereafter, the development of DNA-PK inhibitors and their potential in cancer therapy are reviewed.
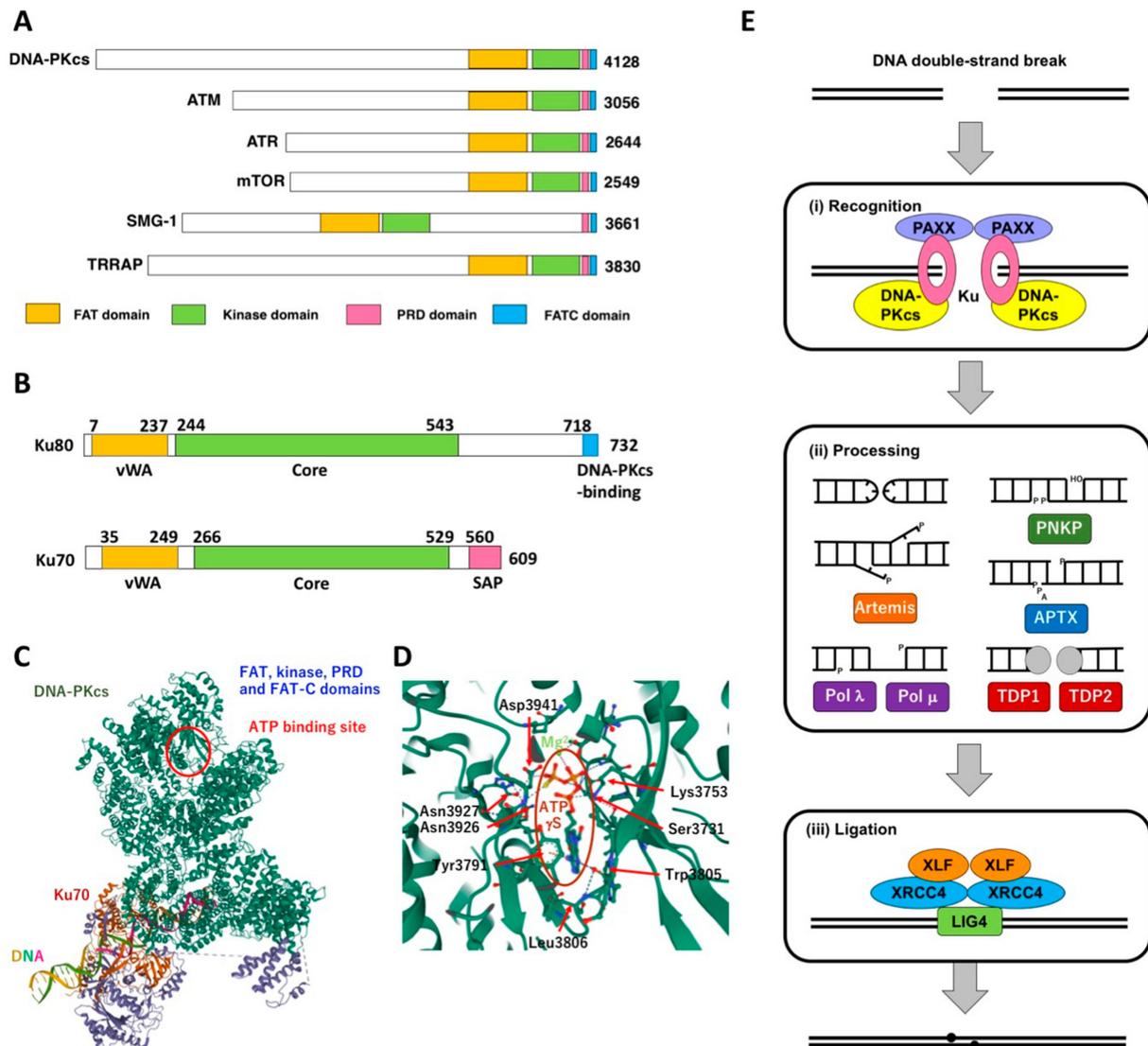
Figure 2. Structure of DNA-PK and its role in NHEJ. (**A**), structure of DNA-PKcs and other PIKK family members. FRAP, ATM and TRRAP (FAT) domain, PIKK-regulatory domain (PRD) and FAT C-terminal (FATC) domains are highlighted. (**B**), structure of Ku80 and Ku70. The von Willebrant factor A (VWA) domain, core domain, SAF-A/B, Acinus and PIAS (SAP) domain and DNA-PKcs binding motif are highlighted. (**C**), the structure of DNA-PKcs complexed with Ku70, Ku80 and dsDNA (RCSB PDB 7K0Y). (**D**), the structure of DNA-PKcs bound to ATPγS (RCSB PDB 7OTP). (**E**), a model for NHEJ. NHEJ proceeds in three stages, (**i**) the recognition stage, (**ii**) the processing stage and (**iii**) the ligation stage. DNA-PK acts in the recognition stage. Figures (**A**,**B**,**E**) are reproduced from our recent reviews [40,59] with some modifications. Figures (**C**,**D**) were drawn using Mol* Viewer [60].

3. Development and Evolution of DNA-PK Inhibitors–Pursuit for Potency and Selectivity

Since the discovery of the importance of DNA-PK in DSB repair through NHEJ, a number of small molecules inhibiting DNA-PK were developed from the 1990s to 2000s. Most of the inhibitors were developed on the basis of the structural similarity of DNA-PK to PI3K. In this phase, high potency, i.e., low 50% inhibiting concentration (IC_{50}), and selectivity, i.e., high IC_{50} for other kinases especially PIKKs and PI3Ks were pursued. Some of the products, such as NU7026 and NU7441, were useful tools for the functional studies on DNA-PK.

3.1. OK-1035

The first reported inhibitor OK-1035, 3-cyano-5-(4-pyridyl)-6-hydrazonomethyl-2-pyridone (Figure 3) was found after screening over 10,000 natural and synthetic compounds [61]. The IC_{50} for DNA-PK activity in vitro was initially reported to be 8 µM [61] but was later reported to be 100 µM [62] (Table 2). OK-1035 retarded the DNA repair in cultured murine leukemia cells at 2 mM [63]. Although the IC_{50} of OK-1035 was at least 100-fold higher for other kinases such as Protein Kinase C, the effects of OK-1035 on PI3Ks and PIKKs were not tested. OK-1035 suppressed the accumulation of p53 and the induction of p21 in response to adriamycin treatment, suggesting that it might have inhibited ATM and/or ATR as well [64].

Table 2. DNA-PK inhibitors with IC_{50} for PIKKs and PI3Ks.

Name of Inhibitor	IC_{50} (nM)								Ref.
	DNA-PK	ATM	ATR	mTOR	PI3Kα	PI3Kβ	PI3Kγ	PI3Kδ	
OK-1035	8000								[61]
	100,000								[62]
Wortmannin	16	150							[65]
	120								[66]
	260	300	4400	2500	3				[67]
LY294002	6000								[67]
	1400	>10,000	>10,000	2800	300	270	3020	220	[68]
NU7026	230	>100,000	>100,000	6400	13,000				[69]
NU7441	14	>100,000	>100,000	1700	5000				[70]
	40	>10,000	>10,000	2400	130	16	220	30	[68]
KU-0060648	185	>3100	>30,000	1800	7800				[71]
	5	>10,000	>10,000	10,000	4	0.5	590	<0.1	[68]
	55	>30,000	>30,000	150	200				[71]
LTURM34	34				>10,000	5,800	>10,000	8500	[72]
NU5455	8.2	>10,000	>10,000	4058	1870	9320	>10,000	276	[73]
IC60211	400								[74]
IC86621	120				1400	135	880	1000	[74]
IC87361	34				3800	1700	800	7900	[74]
AMA37	270	>100,000	>100,000	>100,000	32,000	3700	~100,000	22,000	[75]
Vanillin	1,500,000								[76]
DMNB	15,000								[76]
2-bromo-4,5-dimethoxybenzaldehyde	30,000								[76]
SU11752	130						1100		[77]
PI103	14				2	3	15	3	[78]
NVP-BEZ235	7.5				8	7	15	172	[79]
	1.7				7	72	6	38	[79]
	5	7	21	2	2				[80]
LY3023414	4.24			165	6.07	77.6	23.8	38	[81]
CC-115	13			21	852				[82]
VX-984	115	>30,000	>30,000	>30,000	>20,000	>30,000	7100	>30,000	[71]
M3814	0.6–20	10,000	2800	>10,000	330	250	>1000	95	[83]
	43	>30,000	>30,000	550	800	170	1590	350	[71]
AZD7648 [1]	91.3	17,930	>29,770	>30,000	>8030	>30,000	1370	>30,000	[71]

[1] IC_{50} values for in cellulo phosphorylation of target proteins are shown.
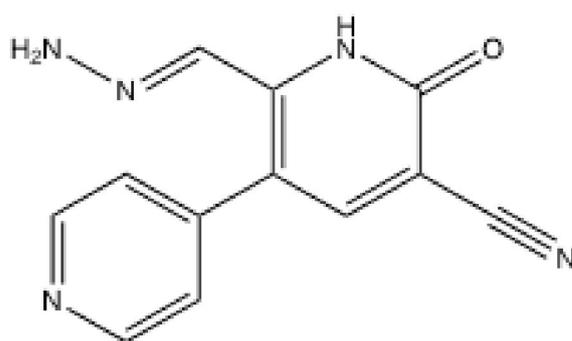
Figure 3. Structure of OK-1035.

3.2. Wortmannin

The findings on the structural similarity of DNA-PK to PI3Ks and PIKKs paved a new avenue toward the development of DNA-PK inhibitors. Wortmannin, [(1R,3R,5S,9R,18S)-18-(methoxymethyl)-1,5-dimethyl-6,11,16-trioxo-13,17-dioxapentacyclo [10.6.1.02,10.05,9.015,19] nonadeca-2(10),12(19),14-trien-3-yl] acetate (Figure 4), which has been known as a PI3K inhibitor [65], was shown to inhibit DNA-PK [11]. Subsequently, ATM was also shown to be sensitive to wortmannin [66]. The IC_{50} of wortmannin for PI3K was 3.0 nM for PI3K [65], 16–120 nM for DNA-PK [67,84], and 100–150 nM for ATM [66,84] (Table 2). Wortmannin did not appreciably affect ATR [84]. Wortmannin was shown to covalently bind to DNA-PKcs [67]. A cryo-EM study, which was published this year, revealed the structure of DNA-PKcs with ATP-γS and four inhibitors, including wortmannin [39]. Wortmannin was shown to occupy the ATP binding site, forming a covalent bond to Lys3753 [39]. A number of studies published in the late 1990s to early 2000s showed that wortmannin augmented IR sensitivity and inhibited DSB repair at 20–50 µM [85,86]. Wortmannin showed radiosensitization on both DNA-PKcs-deficient and ATM-deficient cells [85]. Hence, the radiosensitizing effects of wortmannin are thought to be mediated through multiple mechanisms involving DNA-PK, ATM and PI3Ks.
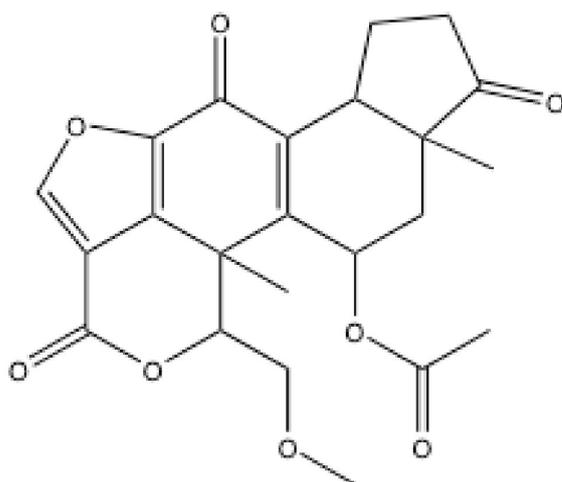

Figure 4. Structure of wortmannin.

3.3. LY294002-Derived Inhibitors

Another PI3K inhibitor LY294002, 2-(4-morpholinyl)-8-phenyl-4H-1-benzopyran-4-one (Figure 5A) [87], was also reported to inhibit DNA-PK [67]. IC_{50} of LY294002 was reported to be 6 µM for DNA-PK [84] and 1.4 µM for PI3K [56] (Table 2). Thus, LY294002 is not a selective inhibitor for DNA-PK, but it led to the discovery of more potent and selective inhibitors of DNA-PK, such as NU7026 and NU7441 (Figure 5). LY294002 was shown to enhance cellular radiosensitivity at 50 µM [85].

By screening a library of LY294002 derivatives, NU7026, 2-(morpholin-4-yl)-benzo[h]
chromen4-one (Figure 5B), was found [69,88]. The IC$_{50}$ of NU7026 for DNA-PK was 230 nM,
which was much lower than that of ATM, ATR, mTOR and PI3K [69,88] (Table 2). The
morpholine ring structure appeared essential for inhibitory activity. NU7026 at 10 μM
sensitized cultured cells to radiation in a manner dependent on DNA-PK [69,88] (Table 3).
NU7026 was also shown to potentiate the cytotoxicity of topoisomerase II poisons [89]. A
preclinical pharmacokinetics study was conducted, showing rapid plasma clearance of
NU7026 through metabolism [90]. Recent studies demonstrated that NU7026 administered
intraperitoneally (i.p.) at 25–50 mg/kg could potentiate the tumor growth suppression via
radiation and chemotherapeutic drugs salinomycin and TRAIL-inducing compound 10
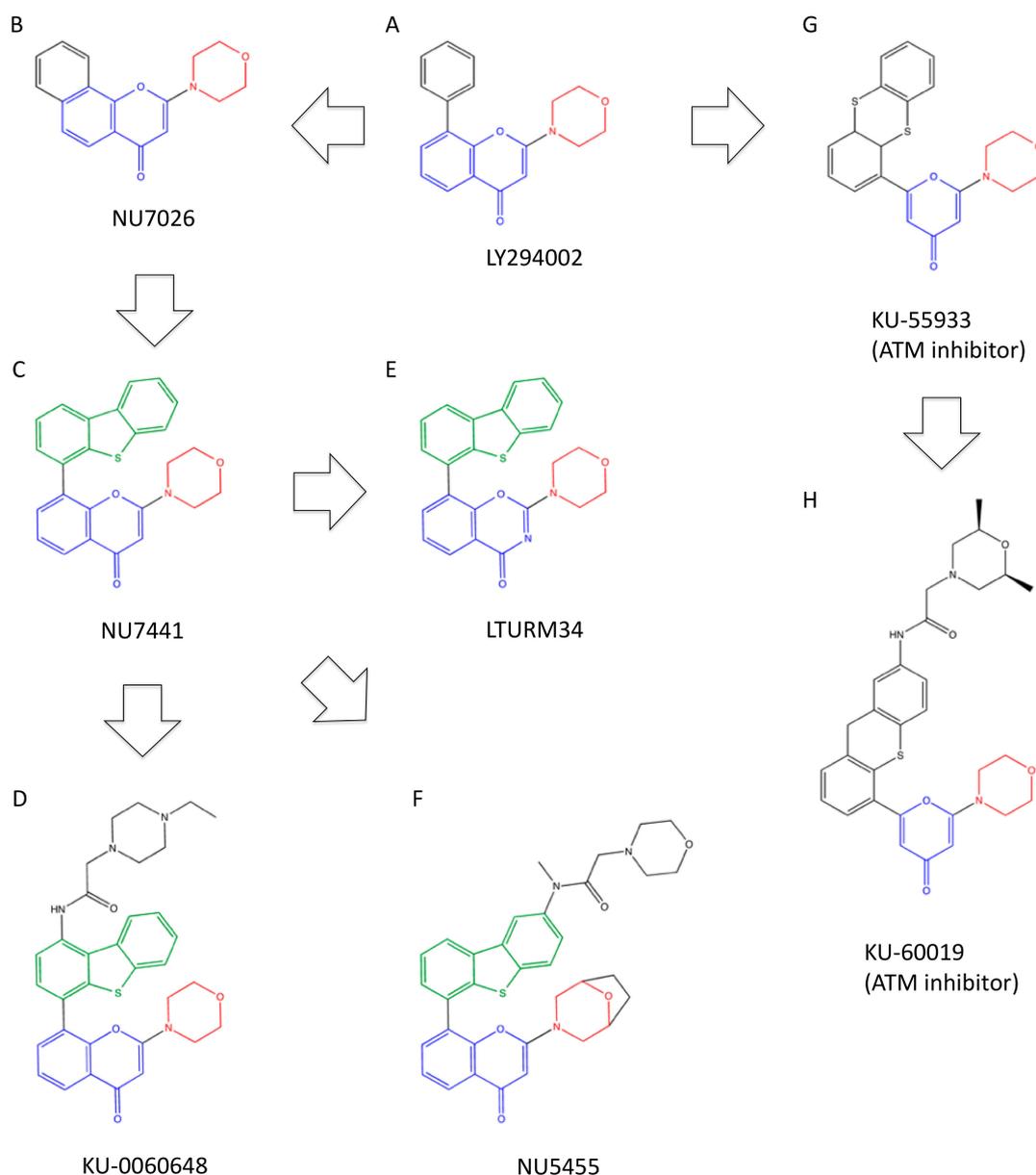(TIC10) in vivo, i.e., in xenograft in immunodeficient mice [91–93] (Table 3).

Figure 5. Structures and mutual relationships of LY294002-derived inhibitors. (**A**) LY294002,
(**B**) NU7026, (**C**) NU7441, (**D**) KU-0060648, (**E**) LTURM34, (**F**) NU5455, (**G**) KU55933,
(**H**) KU-60019. Red: morpholine structures, blue: chromen-4-one or pyran-4-one structures,
green: dibenzothiophen structures.

NU7441, 8-dibenzothiophen-4-yl-2-morpholin-4-yl-chromen-4-one (Figure 5C), showed more potent inhibition of DNA-PK than NU7026 [70,94]. The IC_{50} of NU7441 for DNA-PK was 14 nM [70,94] (Table 2). The latest structural study by cryo-EM showed the insertion of the chromen and morpholine groups into the deepest hydrophobic pocket of DNA-PKcs formed by Leu3751, Tyr3791, Ile3803, Leu3986 and Ile3940 and the insertion of the dibenzothiophene group into another hydrophobic pocket formed by Met3729, Pro3735 and Leu3751 [39]. These multiple interactions between NU7441 and DNA-PKcs would explain the higher affinity and selectivity of NU7441 than wortmannin for DNA-PKcs. To date, NU7441 has been most frequently used in functional studies of DNA-PK. NU7441 sensitized cultured cells to IR and etoposide in a manner dependent on DNA-PKcs at 0.5 µM [95] (Table 3). NU7441, 10–25 mg/kg, i.p., could potentiate tumor growth suppression by radiation and chemotherapeutic drugs in vivo [95,96] (Table 3).

KU-0060648, 2-(4-ethyl-piperazin-1-yl)-N-(4-(2-morpholino-4-oxo-4H-chromen-8-yl)-dibenzo[b,d]thiophen-1-yl)acetamide (Figure 5D), was developed by the modification of NU7441 to increase water solubility [68,97]. KU-0060648 exhibited an IC_{50} of 5 nM for DNA-PK, which is still lower than NU7441 but also inhibited PI3Ks at lower concentrations [68] (Table 2). Hence, KU-0060648 acts as a dual inhibitor for DNA-PK and PI3Ks. Growth inhibition was observed above 30 nM in cultured cancer cell lines and above 10 mg/kg in tumor xenografts [97–99] (Table 3). Sensitization to chemotherapeutic drugs was observed in similar dose ranges [97–99] (Table 3).

LTURM34, 8-(dibenzo[b,d]thiophen-4-yl)-2-morpholino-4H-1,3-benzoxazin-4-one (Figure 5E), in which the chromenone structure in NU7441 was replaced by benzoxazinone, was identified as a more selective inhibitor for DNA-PK [72]. While IC_{50} for DNA-PK was comparable to or higher than NU7441, IC_{50} for PI3Ks was more than two orders of magnitude higher [72] (Table 2). LTURM34 was shown to restore partial chemosensitivity to chemoresistant prostate cancer cells at 3 µM [100] (Table 3).

Recently, another NU7441-derivative NU5455, *N*-(6-(2-(8-oxa-3-azabicyclo [3.2.1]octan-3-yl)-4-oxo-4*H*-chromen-8-yl)dibenzo[b,d]thiophen-2-yl)-N-methyl-2-morpholinoacetamide (Figure 5F), was developed [73]. The IC_{50} of NU5455 for DNA-PK was 8.2 nM but was more than 30-fold higher for PI3Ks [73] (Table 2). In cellulo, NU5455 inhibited DNA-PKcs autophosphorylation with an IC_{50} of 168 nM and increased radiosensitivity and chemosensitivity at concentrations higher than 300 nM [73] (Table 3). Oral (p.o.) administration of NU5455 at 30–100 mg/kg potentiated tumor growth inhibition by radiation and chemotherapeutic agents in vivo (Table 3), notably without adverse effects in normal tissues [73].

It might also be noted that LY294002 was also used to derive ATM inhibitors, KU-55933, 2-morpholin-4-yl-6-thianthren-1-yl-pyran-4-one (Figure 5G) [101], and KU-60019, 2-((2R, 6S)-2,6-Dimethyl-morpholin-4-yl)-N-[5-(6-morpholin-4-yl-4-oxo-4H-pyran-2-yl)-9H-thioxanthen-2-yl]-acetamide (Figure 5H) [102].

Table 3. In cellulo and in vivo radio- or chemo-sensitizing effects of DNA-PK inhibitors.

Name of Inhibitor	In Cellulo Sensitizing Effect					In Vivo Sensitizing Effect				
	Radiation		Chemotherapeutic Drug			Radiation		Chemotherapeutic Drug		
	µM	Ref.	µM	Drug	Ref.	mg/kg [1]	Ref.	mg/kg [1]	Drug	Ref.
NU7026	10	[69]	10	idarubicin, daunorubicin, doxorubicin, etoposide, amsacrine (mAMSA), mitroxantrone	[89]	25, i.p.	[91]	50, i.p.	salinomycin	[92]
								50, i.p.	TIC10 [3]	[93]
NU7441	0.5	[95]	0.5	etoposide	[95]	25, i.p.	[96]	10, i.p.	etoposide	[95]
KU-0060648	0.1	[68]	1	etoposide, doxorubicin	[97]			10, i.p.	etoposide	[97]
			1-10	temozolomide	[99]			10, 50, i.p.	temozolomide	[98]

Table 3. *Cont.*

Name of Inhibitor	In Cellulo Sensitizing Effect					In Vivo Sensitizing Effect				
	Radiation		Chemotherapeutic Drug			Radiation		Chemotherapeutic Drug		
	μM	Ref.	μM	Drug	Ref.	mg/kg [1]	Ref.	mg/kg [1]	Drug	Ref.
LTURM34			3	docetaxel	[100]					
NU5455	1	[73]	1	etoposide, doxorubicin	[73]	30, p.o.	[73]	100, p.o.	etoposide	[73]
								30, p.o.	doxorubicin	[73]
IC86621	50	[74]				400, s.c.	[74]			
IC87361	7	[74]				75 [2], i.p.	[74]			
AMA37	20	[103]								
Vanillin	100, 300	[76]	100	cisplatin	[76]					
DMNB			15	cisplatin	[76]					
SU11752	50	[77]								
PI103	0.06–1	[104]	0.06–1	doxorubicin, etoposide, temozolomide	[104]					
NVP-BEZ235	0.1	[105]				50, 75, p.o.	[106]			
LY3023414								15, p.o.	rapamicin, cisplatin+ gemcitabin	[81]
CC-115	1	[107]								
VX-984	0.1–0.5	[108]				50, p.o.	[108]			
M3814	1	[83]	0.3–0.9	calichiamicin	[109]	5–50, p.o.	[110]	100, p.o.	Mylotarg	[110]
	0.111–1	[110]	0.3	daunorubicin	[111]	50, p.o.	[112]	50, i.g.	paclitaxel, etoposide	[113]
					[113]			50, p.o.	PLD [4]	[114]
	0.5–15	[112]	5	paclitaxel, etoposide		50, p.o.		IR + 5-FU		[115]
						50, p.o.		IR + bintrafusp alpha		[116]
AZD7648	0.1, 1	[71, 117, 118]	0.1	doxorubicin	[71]	50, 100, p.o.	[71]	37.5, 75, p.o.	doxorubicin, olaparib	[71]
						75, p.o.	[117, 118]	100, p.o.	PLD, olaparib	[119]

[1] Abbreviations for the route of administration: i.p., intraperitoneal injection; i.g., intragastrical injection; p.o., per os (oral administration); s.c., subcutaneous injection. [2] Unit: μg/animal. [3] TIC10: TRAIL-inducing compound 10. [4] pegylated liposomal daunorubicin.

3.4. Arylmorpholine-Based Inhibitors

IC60211, 2-hydroxy-4-morpholin-4-yl-benzaldehyde (Figure 6A), was found by screening the small molecular library and showed an IC_{50} of 400 nM for DNA-PK [74] (Table 2). It is noteworthy that this compound also includes a morpholine ring structure, which is similar to LY294002-derived inhibitors. Through the modification of IC60211, more potent and selective inhibitors for DNA-PK, including IC86621, 1-(2-hydroxy-4-morpholin-4-yl-phenyl)-ethanone (Figure 6B), and IC87361, 5-hydroxy-7-morpholino-2-phenyl-4H-chromen-4-one (Figure 6C), were obtained [74]. IC86621 and IC87361 exhibited radiosensitization and chemosensitization concomitantly with reduction in DSB repair ability [74] (Table 3). IC86621 administered subcutaneously (s.c.) at 400 mg/kg and IC87361 administered i.p. at 75 μg per mouse potentiated tumor growth inhibition in vivo [74,120] (Table 3).
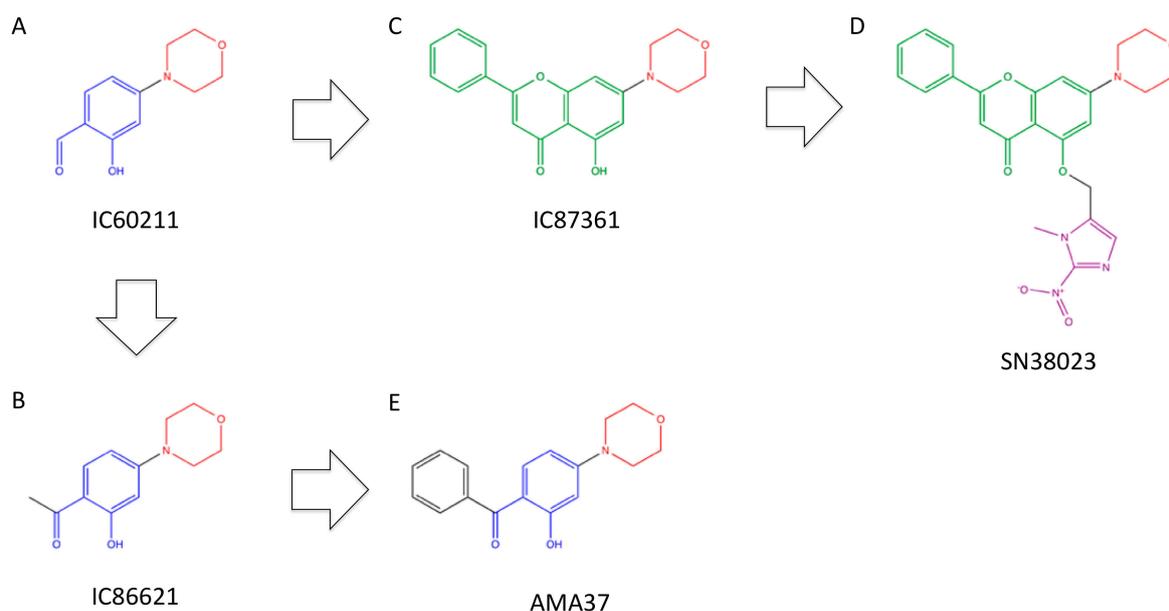
Figure 6. Structures and mutual relationships of arylmorpholine-based inhibitors. (**A**) IC60211, (**B**) IC86621, (**C**) IC87361, (**D**) SN38023, (**E**) AMA37. Red: morpholine structures, blue: o-hydroxybenzaldehyde structures, green: 2-phenyl-4H-chromen-4-one structures, which are common between IC87361 and SN38023, violet: 1-methyl-2-nitro-1H-imidazol-5-yl structure, which is removed in hypoxic conditions.

Recently, SN38023, 5-((1-methyl-2-nitro-1H-imidazol-5-yl)methoxy)-7-morpholino-2-phenyl-4H-chromen-4-one (Figure 6D) was developed [121]. SN38023 itself showed less potent DNA-PK inhibition than IC87361 because of the presence of the nitroimidazole moiety, but it could be metabolized to IC87361 in hypoxic conditions [121]. Thus, SN38023 is expected to act as a prodrug for IC87361, which can target hypoxic tumor cells.

Through testing the arylmorpholine compound library for PI3Ks and PIKKs, AMA37, 1-(2-Hydroxy-4-morpholin-4-yl-phenyl)-phenyl-methanone (Figure 6E), was found as a selective inhibitor for DNA-PK [75] (Table 2). AMA37 showed radiosensitization at 20 μM [103] (Table 3).

3.5. Vanillin-Based Inhibitors

Vanillin, 4-hydroxy-3-methoxybenzoaldehyde (Figure 7A), is a natural product existing in plants such as *Vanilla planifolia*, which is mainly used in food industries as a flavoring agent. Vanillin was shown to inhibit DNA-PK at a high concentration, i.e., $IC_{50} = 1500$ μM [76] (Table 2). Vanillin also inhibited DNA end joining in cell-free extract and sensitized cells to cisplatin [76]. Screening the library of vanillin-related compounds led to the discovery of more potent inhibitors, such as 4,5-dimethoxy-2-nitrobenzaldehyde (DMNB) (Figure 7B) and 2-bromo-4,5-dimethoxybenzaldehyde (Figure 7C), with IC_{50} values of 15 μM and 30 μM, respectively [76] (Table 2). Although the continuous exposure of cells to 100 μM DMNB is toxic to the cells, one hour of treatment significantly increased cellular chemosensitivity [76] (Table 3). Interestingly, a vanillin derivative VND3207, 4-hydroxy-3,5-dimethoxybenzaldehyde (Figure 7D), exerted radioprotective rather than radiosensitizing effects, which was probably through radical scavenging activity and potentiation of DNA-PK activity [122,123].
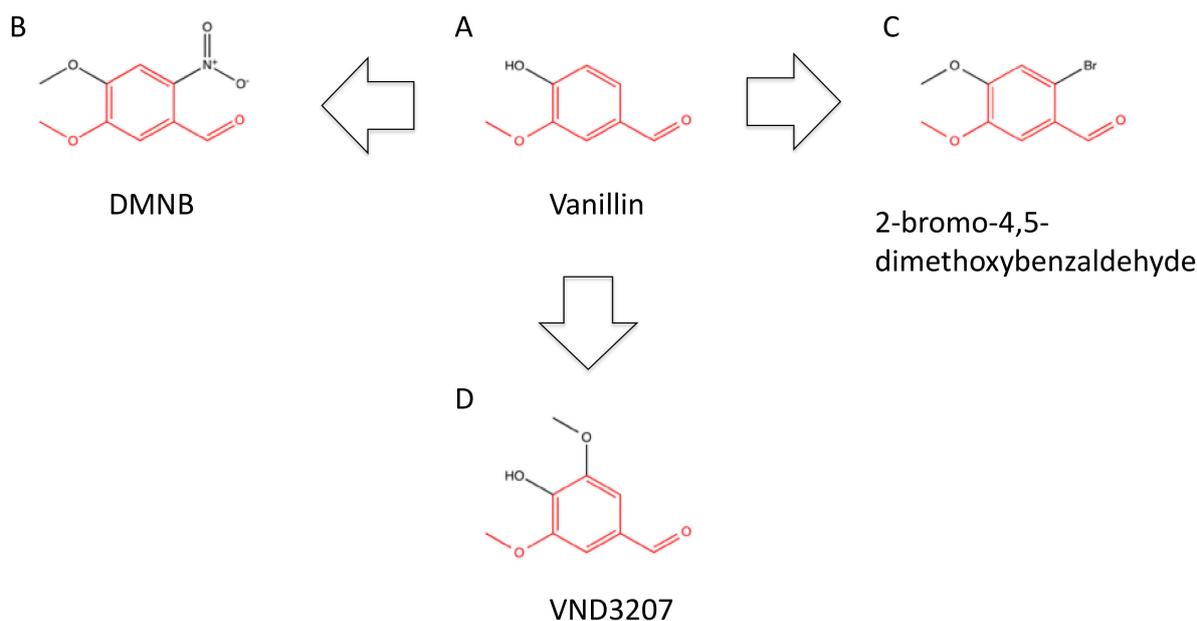
Figure 7. Structure of vanillin-based inhibitors. (**A**) vanillin, (**B**) DMNB, (**C**) 2-bromo-4,5-dimetoxybenzaldehyde, (**D**) VND3207. Meta-methoxy benzaldehyde structures, which are common to all the compounds, are highlighted in red.

3.6. SU11752

SU11752, 5-[[1,2-dihydro-2-oxo-5-[(phenylamino)sulfonyl]-3H-indol-3-ylidene]methyl]-2,4-diethyl-1H-pyrrole-3-propanoic acid (Figure 8), was identified by screening the three-substituted indoline-2-one library. The IC$_{50}$ of SU11752 was comparable to wortmannin for DNA-PK (130 nM) but was higher for PI3K (1.1 μM) [77] (Table 2). Thus, SU11752 is considered a more selective inhibitor for DNA-PK than wortmannin. In cellulo, the inhibition of DSB repair was seen at 12–50 μM and radiosensitization was seen at 50 μM [77] (Table 3).
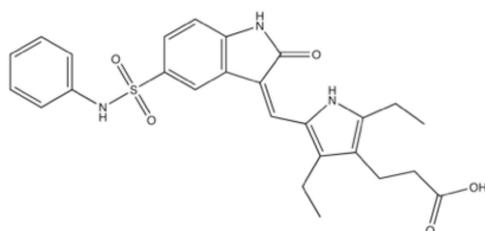
Figure 8. Structure of SU11752.

3.7. PI103

PI103, 2-(3-hydroxyphenyl)-4-morpholinopyrido [30,20:4,5]furo [3,2-d]pyrimidine (Figure 9A), was initially identified as a selective inhibitor for PI3Kα [124] but was subsequently found to inhibit mTOR [78] and DNA-PK as well [79,125]. The IC$_{50}$ of PI103 for DNA-PK was 7.5 nM, which is comparable to that for PI3Kα and PI3Kβ (Table 2). PI103 enhanced the cellular radiosensitivity and chemosensitivity and retarded the DSB repair at 0.06–1 μM [104] (Table 3). Recently, a prodrug of PI103, i.e., RIDR-PI103, 2-amino-N-(5-amino-2-(3-(4-morpholinopyrido [3′,2′:4,5]furo [3,2-d]pyrimidin-2-yl)phenoxy)phenyl) acetamide (Figure 9B) was developed [126,127]. Reactive oxygen species stimulate the intramolecular circularization of this compound, resulting in the release of PI103 [126,127].
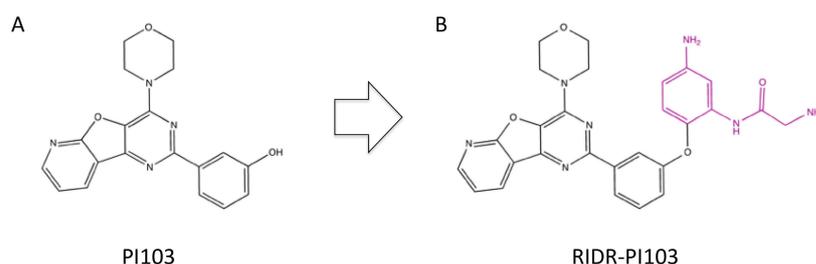
Figure 9. Structure of PI103 (**A**) and RIDR-PI103 (**B**). The phenyl acetamide group, which is removed upon stimulation by reactive oxygen species, is highlighted in violet.

4. Development and Evolution of DNA-PK Inhibitors–Pursuit for Clinical Availability

The potent and selective inhibitors developed above may have been anticipated for applications in cancer therapy, but this was not feasible due to pharmacokinetics and toxicity. In the 2010s, additional inhibitors were developed and are now under clinical trials. Some of them are not selective inhibitors for DNA-PK and are even more inhibitory to mTOR and/or PI3Ks. There are also selective inhibitors for DNA-PK, which are expected to be used in combination with radiation and chemotherapeutic agents. In general, the inhibitors for clinical use show increased solubility in water for oral availability. They also tend to have a large structure and be inserted deeply into the ATP-binding pocket, being in contact as well with amino acids which are not conserved among PIKKs or not in contact with ATP (Figure 2D). Thus, increased contact will enhance the potency and/or selectivity of these inhibitors.

4.1. NVP-BEZ235 (Dactolicib)

NVP-BEZ235, 2-methyl-2-(4-(3-methyl-2-oxo-8-(quinolin-3-yl)-2,3-dihydro-1H-imidaza [4,5-c]quinolin-1-yl)phenyl)propanenitrile (Figure 10A), was initially identified as an orally available inhibitor for PI3K and mTOR [128], but it was found to inhibit DNA-PK, ATM and ATR as well [79,80] (Table 2). NVP-BEZ235 at 100 nM showed more potent radiosensitization and attenuation of DSB repair in comparison to NU7026 and KU55933 at 10 μM [80] (Table 3). Since NVP-BEZ235 could sensitize DNA-PKcs-deficient cells and ATM-deficient cells, radiosensitization might be due to the inhibition of DNA-PK and ATM [105]. NVP-BEZ235 administered p.o. at 50–75 mg/kg potentiated tumor growth inhibition by radiation in vivo [106] (Table 3).
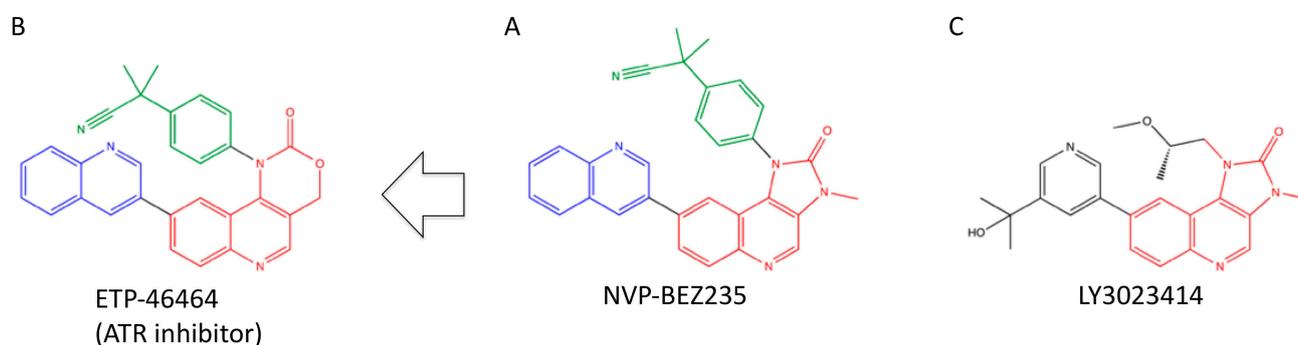

Figure 10. Structures of NVP-BEZ235 (**A**), ETP-46464 (**B**), and LY3023414 (**C**). The imidazoquinoline and oxazinoqinoline structures are highlighted in red. Quinoline and methylphenylpropanenitrile structures, which are common between NVP-BEZ235 and ETP-46464, are highlighted in blue and green, respectively.

Phase 1 and 2 clinical trials are in progress, and the results of eight phase 1 studies and three phase 2 studies have been published to date. Most of these studies have at-

tempted monotherapy, and inhibition of PI3K and/or mTOR rather than DNA-PK may be expected. To date, NVP-BEZ235 has not proven to be satisfactory in therapeutic efficacy and tolerability ([129–131] and others).

ETP-46464, 2-methyl-2-(4-(2-oxo-9-(quinolin-3-yl)-2H-[1,3]oxazino [5,4-c]quinolin-1(4H)-yl)phenyl)propanenitrile (Figure 10B), which has a highly similar structure to NVP-BEZ235, was found as a selective inhibitor for ATR [131].

4.2. LY3023414 (Samotolisib)

LY3023414, 8-[5-(1-hydroxy-1-methylethyl)pyridin-3-yl]-1-[(2S)-2-methoxypropyl]-3-methyl-1,3-dihydro-2H-imidazo [4,5-c]quinolin-2-one (Figure 10C), was developed as a water-soluble and orally available inhibitor for PI3Ks [81]. LY3023414 is structurally similar to NVP-BEZ235. The administration of LY3023414 at 3–30 mg/kg p.o. showed growth inhibition and chemosensitization in vivo [81] (Table 3).

Phase 1 and 2 clinical trials are in progress, and the results of three monotherapeutic phase 1 studies [132–134] and one phase 2 study [135] have been reported to date. There is a report of a phase 1 study combining LY30234014 with Notch inhibitor crenigacestat (LY3039478). In these trials, the inhibition of PI3K and/or mTOR rather than DNA-PK may be expected. Three monotherapeutic phase 1 studies have shown tolerable safety properties with a recommended phase 2 dose (RP2D) of 200 mg administered twice daily (BID) [78,124,125]. In the phase 2 study, recruiting cancer patients with activating PI3K mutations showed only modest clinical activity [135]. The combination of crenigacestat and LY3023414 exhibited poor tolerance, which resulted in lowering the dose and reduced clinical activity [136].

4.3. CC-115

CC-115, 1-Ethyl-7-(2-methyl-6-(1H-1,2,4-triazol-3-yl)pyridin-3-yl)-3,4-dihydropyrazino [2,3-b]pyrazin-2(1H)-one (Figure 11), was found as a dual inhibitor for DNA-PK and mTOR, with IC_{50} of 13 nM and 21 nM, respectively [82] (Table 2). CC-115 inhibited in cellulo the NHEJ of plasmid reporters at 2–6 μM [137] and also sensitized cells to IR at 1 μM [107] (Table 3). It was shown to inhibit the growth of ATM-deficient cells, suggesting possible synthetic lethality by the simultaneous inactivation of DNA-PK and ATM [82]. The administration of CC-115 at 2–5 mg/kg p.o. showed growth inhibition in vivo [138].
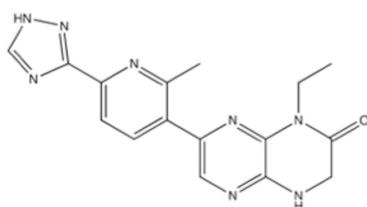

Figure 11. Structure of CC-115.

Phase 1 and 2 clinical trials are in progress, and the results of two phase 1 studies have been published to date, which shows that the administration of 10 mg BID p.o. as monotherapy was tolerable and the clinical activity for advanced solid and hematopoietic malignancies was promising [139,140]. Further clinical studies on the combinatorial treatment with CC-115 and a DNA-damaging anticancer agent may be anticipated.

4.4. VX-984 (M9831)

VX-984, (S)-N-methyl-8-(1-((2'-methyl-[4,5'-bipyrimidin]-6-yl-4',6'-d2)amino)propan-2-yl)quinoline-4-carboxamide (Figure 12), was found to be a potent and selective inhibitor for DNA-PK, although the IC_{50} of VX-984 for DNA-PK, other PIKKs, and PI3Ks in vitro is not described [108,141]. VX-984 was shown to sensitize cultured cells to IR with inhibition of DSB repair at 0.1–0.5 μM and to augment the tumor growth inhibition by radiation in xenograft at 50 mg/kg by p.o. administration in vivo [108,141] (Table 3). Phase 1 and 2

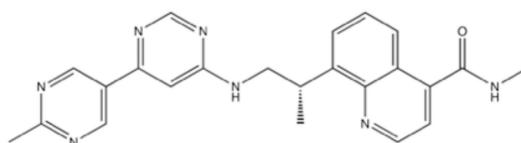clinical trials of VX-984 monotherapy and combination with doxorubicin are currently in progress.

Figure 12. Structure of VX-984.

4.5. M3814 (Peposertib, Nedisertib)

M3814, (S)-[2-chloro-4-fluoro-5-(7-morpholinoquinazolin-4-yl)phenyl]-(6-methoxypyridazin-3-yl)methanol (Figure 13), was discovered through drug library screening at Merck KGaA [83,110]. The IC_{50} for DNA-PKcs was 0.6 nM and 20 nM in the presence of 10 μM or 1 mM ATP, respectively [110] (Table 2). After testing its effects on 284 lipid or protein kinases, only eight showed the IC_{50} values below 1 μM [108]. Thus, M3814 showed high selectivity to DNA-PK. M3814 inhibited DNA-PKcs autophosphorylation of Ser2056 in cellulo at 0.1–1 μM [110]. A recent structural analysis by cryo-EM indicated that morpholine and quinazoline groups fit well to the deepest hydrophobic pocket, similarly to NU7441 (see 3.3) [39]. In addition, its chloro-fluorobenzene ring interacts with Met3729, Ser3731, Pro3735, Leu3751 and Ile3940, and its pyridazine group fits the groove formed by Met3729, Trp3805, Thr 3811, Asn3926 and Met3929, which would stabilize the interaction [39].
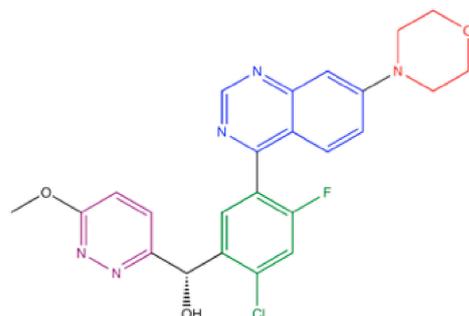

Figure 13. Structure of M3814. Red: morpholine group, blue: quinazoline group, green: chloro-fluorobenzene group, violet: pyridazine group.

M3814 enhanced cellular radiosensitivity in a manner dependent on DNA-PKcs at submicromolar concentration [110] (Table 2). M3814 also sensitized cells to chemotherapeutic agents, such as calicheamicin, microtubule polymerization inhibitor, i.e., paclitaxel, and topoisomerase II inhibitors, i.e., daunorubicin and etoposide [112] (Table 2). Whereas p53-proficient cells undergo cell cycle checkpoint, senescence or apoptosis upon treatment, p53-defcient cells undergo death by mitotic catastrophe [109,111]. Oral or intragastrical (i.g.) administration of M3814 at 5–100 mg/kg augmented tumor growth suppression by radiation and by chemotherapeutic agents, Milotarg (humanized anti-CD33 antibody conjugated to N-acetyl γ-calicheamicin), paclitaxel, etoposide and pegylated liposomal daunorubicin (PLD) in vivo [109–114] (Table 3). One of the latest studies showed that M3814 potentiated the in vivo tumor growth suppression by chemoradiotherapy using 5-fluorouracil [115] and radioimmunotherapy using bintrafusp α, which inhibit profibroblasitic TGFβ and immunosuppressive PD-L1 [116]. M3814 was also shown to bind to ATP-binding cassette transporter family G2 (ABCG2) and reverse drug resistance [142].

In a phase 1 study, M3814 was well tolerated with RP2D of 400 mg BID [143]. Concentration-dependent reduction in DNA-PKcs autophosphorylation in peripheral blood mononuclear cells was also observed [143]. Although M3814 monotherapy did not show partial response in this study [143], the combination with radiotherapy or chemotherapy is currently under phase 1 clinical trial, and the results are anticipated.

4.6. AZD7648

AZD7648, 7-methyl-2-[(7-methyl [1,2,4]triazolo [1,5-a]pyridin-6-yl)amino]-9-(tetrahydro-2H-pyran-4-yl)-7,9-dihydro-8H-purin-8-one (Figure 14), was identified by library screening followed by optimization in AstraZeneka [71,144]. In a panel of 397 kinases, only DNA-PK, PI3Kα, PI3Kβ and PI3Kδ showed >50% inhibition at 1 μM [71]. The IC$_{50}$ for in vitro DNA-PK was 0.6 nM and that for in cellulo DNA-PKcs Ser2056 autophosphorylation was 91.3 nM [71] (Table 2). In the latest structural analysis by cryo-EM, the triazopyrimidine group was fitted into the deepest hydrophobic pocket, as in the case of NU7441 and M3814 [39]. Furthermore, the purinone group docked the hydrophobic tunnel formed by Trp3805, Leu 3806 and Met 3829 and was placed mostly parallel with the indole ring of Trp3805, forming π stacking, which might further stabilize the interaction between AZD7648 and DNA-PKcs [39].
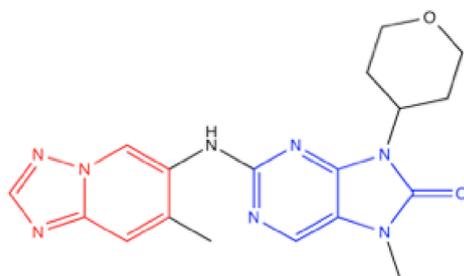

Figure 14. Structure of AZD7648. Red: triazopyrimidine structure, blue: purinone structure.

AZD7648 sensitized cells to IR and doxorubicin at submicromolar concentrations [71] (Table 3). Oral administration of AZD7648 at 37.5–100 mg/kg potentiated tumor growth inhibition by radiation, doxorubicin and olaparib, PARP inhibitor, in vivo [71,117–119] (Table 3). It is notable that AZD7648 enhanced the olaparib sensitivity of ATM-deficient cells [71]. This is in contrast to earlier studies showing that the absence or inhibition of DNA-PK, using NU7441 or KU-0060648, alleviated the toxicity of olaparib on ATM-deficient cells [145,146].

Phase 1 and 2 clinical trials of AZD7648 monotherapy and its combination with doxorubicin or olaparib are currently in progress.

5. Summary and Future Directions

As seen above, a number of DNA-PK inhibitors have been developed. Potent and selective inhibitors in the earlier generation, such as NU7026 and NU7441, have been useful tools in functional studies of DNA-PK. In the next generation, dual inhibitors such as LY3023414 and CC-115, and DNA-PK-selective inhibitors such as VX-984, M3814 and AZD7648, have promising effects in preclinical studies and are now under clinical trials. The development of these inhibitors in the 1990s and 2000s was greatly promoted by the systematic chemical modification of previously identified PI3K inhibitors to increase the potency and selectivity toward DNA-PK. On the other hand, M3814 and AZD7648 were found recently through large-scale de novo screening, underscoring the importance of this approach. The latest study elucidating the structure of the complex of DNA-PKcs and inhibitors indicated a possibility of structure-guided drug development.

Dual inhibitors LY3023414 and CC-115 have exhibited growth inhibitory effects in monotherapy as seen in preclinical studies. On the other hand, VX-984, M3814 and AZD7648 showed modest growth inhibition at most but potent sensitization to IR and DNA-damaging chemotherapeutic agents. Thus, the growth inhibition by dual inhibitor may be due primarily to the inhibition of PI3K/mTOR. In order to utilize the potential of dual inhibitors in inhibiting DNA-PK, future studies on the combination with radiotherapy and/or chemotherapy are anticipated.

Recent preclinical studies of M3814 and AZD7648 indicate promising combinations. M3814 showed enhancement of the efficacy of chemoradiotherapy and radioimmunother-

apy. AZD7648 potentiated the effects of olaparib, especially to a great extent in ATM-deficient cells. There are lines of evidence indicating that the carriers of pathogenic ATM mutation, accounting for 1–2% in human populations, exhibit a several-fold increased risk of breast cancer [147,148]. Since ATM plays a pleiotropic role in the maintenance of the genome, elevated cancer risk may be caused by haploinsufficiency or the second hit, i.e., the loss of the active allele. It is assumed in the latter case that cancer cells have lost ATM function, whereas normal cells retain it. The cancer cells would then be selectively sensitized to the combination of olaparib and DNA-PK inhibitor. Further studies may be warranted to explore the effects of other combinations and in other genetic statuses.

Conflicts of Interest: The authors declare no conflict of interest.

References

1. United Nations Scientific Committee on the Effects of Atomic Radiation. *Report of the United Nations Scientific Committee on the Effects of Atomic Radiation 2010 Fifty-Seventh Session, Includes Scientific Report: Summary of Low-Dose Radiation Effects on Health*; United Nations Scientific Committee on the Effects of Atomic Radiation: Vienna, Austria, 2010.
2. Zhao, B.; Rothenberg, E.; Ramsden, D.A.; Lieber, M.R. The molecular basis and disease relevance of non-homologous DNA end joining. *Nat. Rev. Mol. Cell Biol.* **2020**, *21*, 765–781. [CrossRef] [PubMed]
3. Yilmaz, D.; Furst, A.; Meaburn, K.; Lezaja, A.; Wen, Y.; Altmeyer, M.; Reina-San-Martin, B.; Soutoglou, E. Activation of homologous recombination in G1 preserves centromeric integrity. *Nature* **2021**, *600*, 748–753. [CrossRef]
4. Dvir, A.; Stein, L.Y.; Calore, B.L.; Dynan, W.S. Purification and characterization of a template-associated protein kinase that phosphorylates RNA polymerase II. *J. Biol. Chem.* **1993**, *268*, 10440–10447. [CrossRef]
5. Gottlieb, T.M.; Jackson, S.P. The DNA-dependent protein kinase: Requirement for DNA ends and association with Ku antigen. *Cell* **1993**, *72*, 131–142. [CrossRef]
6. Hartley, K.; Gell, D.; Smith, C.; Zhang, H.; Divecha, N.; Connelly, M.; Admon, A.; Lees-Miller, S.; Anderson, C.; Jackson, S. DNA-dependent protein kinase catalytic subunit: A relative of phosphatidylinositol 3-kinase and the ataxia telangiectasia gene product. *Cell* **1995**, *82*, 849–856. [CrossRef]
7. Savitsky, K.; Bar-Shira, A.; Gilad, S.; Rotman, G.; Ziv, Y.; Vanagaite, L.; Tagle, D.A.; Smith, S.; Uziel, T.; Sfez, S.; et al. A single ataxia telangiectasia gene with a product similar to PI-3 kinase. *Science* **1995**, *268*, 1749–1753. [CrossRef] [PubMed]
8. Bentley, N.J.; Holtzman, D.A.; Flaggs, G.; Keegan, K.S.; DeMaggio, A.; Ford, J.C.; Hoekstra, M.; Carr, A.M. The Schizosaccharomyces pombe rad3 checkpoint gene. *EMBO J.* **1996**, *15*, 6641–6651. [CrossRef]
9. Cimprich, K.A.; Shin, T.B.; Keith, C.T.; Schleiber, S.L. cDNA cloning and gene mapping of a candidate human cell cycle checkpoint protein. *Proc. Natl. Acad. Sci. USA* **1996**, *93*, 2850–2855. [CrossRef]
10. Girard, P.M.; Riballo, E.; Begg, A.C.; Waugh, A.; Jeggo, P.A. Nbs1 promotes ATM dependent phosphorylation events including those required for G1/S arrest. *Oncogene* **2002**, *21*, 4191–4199. [CrossRef]
11. Uziel, T.; Lerenthal, Y.; Moyal, L.; Andegeko, Y.; Mittelman, L.; Shiloh, Y. Requirement of the MRN complex for ATM activation by DNA damage. *EMBO J.* **2003**, *22*, 5612–5621. [CrossRef]
12. Zou, L.; Elledge, S.J. Sensing DNA damage through ATRIP recognition of RPA-ssDNA complexes. *Science* **2003**, *300*, 1542–1548. [CrossRef]
13. Brown, E.J.; Albers, M.W.; Shin, T.B.; Ichikawa, K.; Keith, C.T.; Lane, W.S.; Schreiber, S.L. A mammalian protein targeted by G1-arresting rapamycin-receptor complex. *Nature* **1994**, *369*, 756–758. [CrossRef]
14. Sabatini, D.M.; Erdjument-Bromage, H.; Lui, M.; Tempst, P.; Snyder, S.H. RAFT1: A mammalian protein that binds to FKBP12 in a Rapamycin-dependent fashion and is homologous to yeast TORs. *Cell* **1994**, *78*, 35–43. [CrossRef]
15. Denning, G.; Jamieson, L.; Maquat, L.E.; Thompson, E.A.; Fields, A.P. Cloning of a novel phosphatidylinositol kinase-related kinase: Characterization of the human SMG-1 RNA surveillance protein. *J. Biol. Chem.* **2001**, *276*, 22709–22714. [CrossRef]
16. Yamashita, A.; Ohnishi, T.; Kashima, I.; Taya, Y.; Ohno, S. Human SMG-1, a novel phosphatidylinositol 3-kinase-related protein kinase, associates with components of the mRNA surveillance complex and is involved in the regulation of nonsense-mediated mRNA decay. *Genes Dev.* **2001**, *15*, 2215–2228. [CrossRef]
17. McMahon, S.B.; Van Buskirk, H.A.; Dugan, K.A.; Copeland, T.D.; Cole, M.D. The novel ATM-related protein TRRAP is an essential cofactor for the c-Myc and E2F oncoproteins. *Cell* **1998**, *94*, 363–374. [CrossRef]

18. Alemi, F.; Sadigh, A.R.; Malakoti, F.; Elhaei, Y.; Ghaffari, S.H.; Maleki, M.; Asemi, Z.; Yousefi, B.; Targhazeh, N.; Majidinia, M. Molecular mechanisms involved in DNA repair in human cancers: An overview of PI3k/Akt signaling and PIKKs crosstalk. *J. Cell Phisiol.* **2022**, *237*, 313–328. [CrossRef]

19. Huang, T.T.; Lampert, E.J.; Coots, C.; Lee, J.M. Targeting the PI3K pathway and DNA damage response as a therapeutic strategy in ovarian cancer. *Cancer Treat. Rev.* **2020**, *86*, 102021. [CrossRef]

20. Wanigasooriya, K.; Tyler, R.; Barros-Silva, J.D.; Sinha, Y.; Ismail, T.; Beggs, A.D. Radiosensitising Cancer Using Phosphatidylinositol-3-Kinase (PI3K), Protein Kinase B (AKT) or Mammalian Target of Rapamycin (mTOR) Inhibitors. *Cancers (Basel)* **2020**, *12*, 1278. [CrossRef]

21. Gewandter, J.S.; Bambara, R.A.; O'Reilly, M.A. The RNA surveillance protein SMG1 activates p53 in response to DNA double-strand breaks but not exogenously oxidized mRNA. *Cell Cycle* **2011**, *10*, 2561–2567. [CrossRef]

22. Gubanova, E.; Issaeva, N.; Gokturk, C.; Djureinovic, T.; Helleday, T. SMG-1 suppresses CDK2 and tumor growth by regulating both the p53 and Cdc25A signaling pathways. *Cell Cycle* **2013**, *12*, 3770–3780. [CrossRef] [PubMed]

23. Zhang, C.; Mi, J.; Deng, Y.; Deng, Z.; Long, D.; Liu, Z. DNMT1 Enhances the Radiosensitivity of HPV-Positive Head and Neck Squamous Cell Carcinomas via Downregulating SMG1. *Onco. Targets Ther.* **2020**, *13*, 4201–4211. [CrossRef] [PubMed]

24. Long, D.; Xu, L.; Deng, Z.; Guo, D.; Zhang, Y.; Liu, Z.; Zhang, C. HPV16 E6 enhances the radiosensitivity in HPV-positive human head and neck squamous cell carcinoma by regulating the miR-27a-3p/SMG1 axis. *Infect. Agent Cancer* **2021**, *16*, 56. [CrossRef] [PubMed]

25. Chen, Y.H.; Wei, M.F.; Wang, C.W.; Lee, H.W.; Pan, S.L.; Gao, M.; Kuo, S.H.; Cheng, A.L.; Teng, C.M. Dual phosphoinositide 3-kinase/mammalian target of rapamycin inhibitor is an effective radiosensitizer for colorectal cancer. *Cancer Lett.* **2015**, *357*, 582–590. [CrossRef]

26. Del Peso, L.; González-García, M.; Page, C.; Herrera, R.; Nuñez, G. Interleukin-3-induced phosphorylation of BAD through the protein kinase Akt. *Science* **1997**, *278*, 687–689. [CrossRef]

27. Datta, S.R.; Dudek, H.; Tao, X.; Masters, S.; Fu, H.; Gotoh, Y.; Greenberg, M.E. Akt phosphorylation of BAD couples survival signals to the cell-intrinsic death machinery. *Cell* **1997**, *91*, 231–241. [CrossRef]

28. Zhou, B.P.; Liao, Y.; Xia, W.; Zou, Y.; Spohn, B.; Hung, M.C. HER-2/neu induces p53 ubiquitination via Akt-mediated MDM2 phosphorylation. *Nat. Cell Biol.* **2001**, *3*, 973–982. [CrossRef]

29. Oeck, S.; Al-Refae, K.; Riffkin, H.; Wiel, G.; Handrick, R.; Klein, D.; Iliakis, G.; Jendrossek, V. Activating Akt1 mutations alter DNA double strand break repair and radiosensitivity. *Sci. Rep.* **2017**, *7*, 42700. [CrossRef]

30. Mueck, K.; Rebholz, S.; Harati, M.D.; Rodemann, H.P.; Toulany, M. Akt1 Stimulates Homologous Recombination Repair of DNA Double-Strand Breaks in a Rad51-Dependent Manner. *Int. J. Mol. Sci.* **2017**, *18*, 2473. [CrossRef]

31. Bozulic, L.; Surucu, B.; Hynx, D.; Hemmings, B.A. PKBalpha/Akt1 acts downstream of DNA-PK in the DNA double-strand break response and promotes survival. *Mol. Cell* **2008**, *30*, 203–213. [CrossRef]

32. Liu, L.; Dai, X.; Yin, S.; Liu, P.; Hill, E.G.; Wei, W.; Gan, W. DNA-PK promotes activation of the survival kinase AKT in response to DNA damage through an mTORC2-ECT2 pathway. *Sci. Signal* **2022**, *15*, eabh2290. [CrossRef]

33. Yaneva, M.; Wen, J.; Ayala, A.; Cook, R. cDNA-derived amino acid sequence of the 86-kDa subunit of the Ku antigen. *J. Biol. Chem.* **1989**, *264*, 13407–13411. [CrossRef]

34. Reeves, W.H.; Sthoeger, Z.M. Molecular cloning of cDNA encoding the p70 (Ku) lupus autoantigen. *J. Biol. Chem.* **1989**, *264*, 5047–5052. [CrossRef]

35. Mimori, T.; Hardin, J.A. Mechanism of interaction between Ku protein and DNA. *J. Biol. Chem.* **1986**, *261*, 10375–10379. [CrossRef]

36. Falck, J.; Coates, J.; Jackson, S.P. Conserved modes of recruitment of ATM, ATR and DNA-PKcs to sites of DNA damage. *Nature* **2005**, *434*, 605–611. [CrossRef]

37. Walker, J.R.; Corpina, R.A.; Goldberg, J. Structure of the Ku heterodimer bound to DNA and its implication for double-strand break repair. *Nature* **2001**, *412*, 607–614. [CrossRef]

38. Chen, X.; Xu, X.; Chen, Y.; Cheung, J.C.; Wang, H.; Jiang, J.; de Val, N.; Fox, T.; Gellert, M.; Yang, W. Structure of an activated DNA-PK and its implications for NHEJ. *Mol. Cell* **2021**, *81*, 801–810. [CrossRef]

39. Liang, S.; Thomas, S.E.; Chaplin, A.K.; Hardwick, S.W.; Chirgadze, D.Y.; Blundell, T.L. Structural insights into inhibitor regulation of the DNA repair protein DNA-PKcs. *Nature* **2022**, *601*, 643–648. [CrossRef]

40. Matsumoto, Y.; Asa, A.D.D.C.; Modak, C.; Shimada, M. DNA-dependent protein kinase catalytic subunit: The sensor for DNA double-strand breaks structurally and functionally related to Ataxia telangiectasia mutated. *Genes* **2021**, *12*, 1143.

41. Taccioli, G.E.; Gottlieb, T.M.; Blunt, T.; Priestley, A.; Demengeot, J.; Mizuta, R.; Lehmann, A.R.; Alt, F.W.; Jackson, S.P.; Jeggo, P.A. Ku80: Product of the XRCC5 gene and its role in DNA repair and V(D)J recombination. *Science* **1994**, *265*, 1442–1445. [CrossRef]

42. Smider, V.; Rathmell, W.K.; Lieber, M.R.; Chu, G. Restoration of X-ray resistance and V(D)J recombination in mutant cells by Ku cDNA. *Science* **1994**, *266*, 288–291. [CrossRef]

43. Blunt, T.; Finnie, N.J.; Taccioli, G.E.; Smith, G.C.; Demengeot, J.; Gottlieb, T.M.; Mizuta, R.; Varghese, A.J.; Alt, F.W.; Jeggo, P.A. Defective DNA-dependent protein kinase activity is linked to V(D)J recombination and DNA repair defects associated with the murine scid mutation. *Cell* **1995**, *80*, 813–823. [CrossRef]

44. Kirchgessner, C.U.; Patil, C.K.; Evans, J.W.; Cuomo, C.A.; Fried, L.M.; Carter, T.; Oettinger, M.A.; Brown, J.M. DNA-dependent kinase (p350) as a candidate gene for the murine SCID defect. *Science* **1995**, *267*, 1178–1183. [CrossRef]

45. Peterson, S.R.; Kurimasa, A.; Oshimura, M.; Dynan, W.S.; Bradbury, E.M.; Chen, D.J. Loss of the catalytic subunit of the DNA-dependent protein kinase in DNA double-strand-break-repair mutant mammalian cells. *Proc. Natl. Acad. Sci. USA* **1995**, *92*, 3171–3174. [CrossRef]

46. Ochi, T.; Blackford, A.N.; Coates, J.; Jhujh, S.; Mehmood, S.; Tamura, N.; Travers, J.; Wu, Q.; Draviam, V.M.; Robinson, C.V.; et al. DNA repair. PAXX, a paralog of XRCC4 and XLF, interacts with Ku to promote DNA double-strand break repair. *Science* **2015**, *347*, 185–188. [CrossRef]

47. Xing, M.; Yang, M.; Huo, W.; Feng, F.; Wei, L.; Jiang, W.; Ning, S.; Yan, Z.; Li, W.; Wang, Q.; et al. Interactome analysis identifies a new paralogue of XRCC4 in non-homologous end joining DNA repair pathway. *Nat. Commun.* **2015**, *6*, 6233. [CrossRef]

48. Craxton, A.; Somers, J.; Munnur, D.; Jukes-Jones, R.; Cain, K.; Malewicz, M. XLS (c9orf142) is a new component of mammalian DNA double-stranded break repair. *Cell Death Diff.* **2015**, *22*, 890–897. [CrossRef]

49. Moshous, D.; Callebaut, I.; de Chasseval, R.; Corneo, B.; Cavazzana-Calvo, M.; Le Deist, F.; Tezcan, I.; Sanal, O.; Bertrand, Y.; Philippe, N.; et al. Artemis, a novel DNA double-strand break repair/V(D)J recombination protein, is mutated in human severe combined immune deficiency. *Cell* **2001**, *105*, 177–186. [CrossRef]

50. Ma, Y.; Pannicke, U.; Schwarz, K.; Lieber, M.R. Hairpin opening and overhang processing by an Artemis/DNA-dependent protein kinase complex in nonhomologous end joining and V(D)J recombination. *Cell* **2002**, *108*, 781–794. [CrossRef]

51. Li, Z.; Otevrel, T.; Gao, Y.; Cheng, H.; Seed, B.; Stamato, T.; Taccioli, G.E.; Alt, F.W. The XRCC4 gene encodes a novel protein involved in DNA double-strand break repair and V(D)J recombination. *Cell* **1995**, *83*, 1079–1089. [CrossRef]

52. Critchlow, S.; Bowater, R.; Jackson, S. Mammalian DNA double-strand break repair protein XRCC4 interacts with DNA ligase IV. *Curr. Biol.* **1997**, *7*, 588–598. [CrossRef]

53. Grawunder, U.; Wilm, M.; Wu, X.; Kulesza, P.; Wilson, T.; Mann, M.; Leiber, M.R. Activity of DNA ligase IV stimulated by complex formation with XRCC4 protein in mammalian cells. *Nature* **1997**, *388*, 492–495. [PubMed]

54. Buck, D.; Malivert, L.; de Chasseval, R.; Barraud, A.; Fondanèche, M.C.; Sanal, O.; Plebani, A.; Stéphan, J.L.; Hufnagel, M.; le Deist, F.; et al. Cernunnos, a novel nonhomologous end-joining factor, is mutated in human immunodeficiency with microcephaly. *Cell* **2006**, *124*, 287–299. [CrossRef] [PubMed]

55. Ahnesorg, P.; Smith, P.; Jackson, S.P. XLF interacts with the XRCC4-DNA ligase IV complex to promote DNA nonhomologous end-joining. *Cell* **2006**, *124*, 301–313. [CrossRef]

56. Hammel, M.; Yu, Y.; Fang, S.; Lees-Miller, S.P.; Tainer, J.A. XLF regulates filament architecture of the XRCC4·ligase IV complex. *Structure* **2010**, *18*, 1431–1442. [CrossRef]

57. Kienker, L.J.; Shin, E.K.; Meek, K. Both V(D)J recombination and radioresistance require DNA-PK kinase activity, though minimal levels suffice for V(D)J recombination. *Nucleic Acids Res.* **2000**, *28*, 2752–2761. [CrossRef]

58. Kurimasa, A.; Kumano, S.; Boubnov, N.; Story, M.; Tung, C.; Peterson, S.; Chen, D.J. Requirement for the kinase activity of human DNA-dependent protein kinase catalytic subunit in DNA strand break rejoining. *Mol. Cell Biol.* **1999**, *19*, 3877–3884. [CrossRef]

59. Matsumoto, Y.; Sharma, M.K. DNA-dependent protein kinase in DNA damage response: Three decades and beyond. *J. Radiat. Cancer Res.* **2020**, *11*, 123–134. [CrossRef]

60. Sehnal, D.; Bittrich, S.; Deshpande, M.; Svobodová, R.; Berka, K.; Bazgier, V.; Velankar, S.; Burley, S.K.; Koča, J.; Rose, A.S. Mol* Viewer: Modern web app for 3D visualization and analysis of large biomolecular structures. *Nucleic Acids Res.* **2021**, *49*, 431–437. [CrossRef]

61. Take, Y.; Kumano, M.; Hamano, Y.; Fukatsu, H.; Teraoka, H.; Nishimura, S.; Okumura, A. OK-1035, a selective inhibitor of DNA-dependent protein kinase. *Biochem. Biophys. Res. Commun.* **1995**, *215*, 41–47. [CrossRef]

62. Stockley, M.; Clegg, W.; Fontana, G.; Golding, B.T.; Martin, N.; Rigoreau, L.J.; Smith, G.C.; Griffin, R.J. Synthesis, crystal structure determination, and biological properties of the DNA-dependent protein kinase (DNA-PK) inhibitor 3-cyano-6-hydrazonomethyl-5-(4-pyridyl)prid-[1H]-2-one (OK-1035). *Bioorg. Med. Chem. Lett.* **2001**, *11*, 2837–2841. [CrossRef]

63. Kruszweski, M.; Wojewódzka, M.; Iwaneńko, T.; Szumiel, I.; Okuyama, A. Differential inhibitory effect of OK-1035 on DNA repair in L5178Y murine lymphoma sublines with functional or defective repair of double strand breaks. *Mutat. Res.* **1998**, *409*, 31–36. [CrossRef]

64. Take, Y.; Kumano, M.; Teraoka, H.; Nishimura, S.; Okuyama, A. DNA-dependent protein kinase inhibitor (OK-1035) suppresses p21 expression in HCT116 cells containing wild-type p53 induced by adriamycin. *Biochem. Biophys. Res. Commun.* **1996**, *221*, 207–212. [CrossRef]

65. Yano, H.; Nakanishi, S.; Kimura, K.; Hanai, N.; Saitoh, Y.; Fukui, Y.; Nonomura, Y.; Matsuda, Y. Inhibition of histamine secretion by wortmannin through the blockade of phosphatidylinositol 3-kinase in RBL-2H3 cells. *J. Biol. Chem.* **1993**, *268*, 25846–25856. [CrossRef]

66. Banin, S.; Moyal, L.; Shieh, S.-Y.; Taya, Y.; Anderson, C.W.; Chessa, L.; Smorodinsky, N.I.; Prives, C.; Reiss, Y.; Shiloh, Y.; et al. Enhanced phosphorylation of p53 by ATM in response to DNA damage. *Science* **1998**, *281*, 1674–1677. [CrossRef]

67. Izzard, R.A.; Jackson, S.P.; Smith, G.C.M. Competitive and noncompetitive inhibition of the DNA-dependent protein kinase. *Cancer Res.* **1999**, *59*, 2581–2586.

68. Cano, C.; Saravanan, K.; Bailey, C.; Bardos, J.; Curtin, N.J.; Frigerio, M.; Golding, B.T.; Hardcastle, I.R.; Hummersone, M.G.; Menear, K.A.; et al. 1-substituted (Dibenzo[b,d]thiophen-4-yl)-2-morpholino-4H-chromen-4-ones endowed with dual DNA-PK/PI3-K inhibitory activity. *J. Med. Chem.* **2013**, *56*, 6386–6401. [CrossRef]

69. Veuger, S.J.; Curtin, N.J.; Richardson, C.J.; Smith, G.C.M.; Durkacz, B.W. Radiosensitization and DNA Repair Inhibition by the Combined Use of Novel Inhibitors of DNA-dependent Protein Kinase and Poly(ADP-Ribose) Polymerase-1. *Cancer Res.* **2003**, *63*, 6008–6015.

70. Leahy, J.J.J.; Golding, B.T.; Griffin, R.J.; Hardcastle, I.R.; Richardson, C.; Rigoreau, L.; Smith, G.C.M. Identification of a highly potent and selective DNA-dependent protein kinase (DNA-PK) inhibitor (NU7441) by screening of chromenone libraries. *Bioorg. Med. Chem. Lett.* **2004**, *14*, 6083–6087. [CrossRef]

71. Fok, J.H.L.; Ramos-Montoya, A.; Vazquez-Chantada, M.; Wijnhoven, P.W.G.; Follia, V.; James, N.; Farrington, P.M.; Karmokar, A.; Willis, S.E.; Cairns, J.; et al. AZD7648 is a potent and selective DNA-PK inhibitor that enhances radiation, chemotherapy and olaparib activity. *Nat. Commun.* **2019**, *10*, 5065. [CrossRef]

72. Morrison, R.; Al-Rawi, J.M.; Jennings, I.G.; Thompson, P.E.; Angove, M.J. Synthesis, structure elucidation, DNA-PK and PI3K and anti-cancer activity of 8- and 6-aryl-substituted-1-3-benzoxazines. *Eur. J. Med. Chem.* **2016**, *110*, 326–339. [CrossRef] [PubMed]

73. Willoughby, C.E.; Jiang, Y.; Thomas, H.D.; Willmore, E.; Kyle, S.; Wittner, A.; Phillips, N.; Zhao, Y.; Tudhope, S.J.; Prendergast, L.; et al. Selective DNA-PKcs inhibition extends the therapeutic index of localized radiotherapy and chemotherapy. *J. Clin. Investig.* **2020**, *130*, 258–271. [CrossRef] [PubMed]

74. Kashishian, A.; Douangpanya, H.; Clark, D.; Schlachter, S.T.; Eary, C.T.; Schiro, J.G.; Huang, H.; Burgess, L.E.; Kesicki, E.A.; Halbrook, J. DNA-dependent protein kinase inhibitors as drug candidates for the treatment of cancer. *Mol. Cancer Ther.* **2003**, *2*, 1257–1264. [PubMed]

75. Knight, Z.A.; Chiang, G.G.; Alaimo, P.J.; Kenski, D.M.; Ho, C.B.; Coan, K.; Abraham, R.T.; Shokat, K.M. Isoform-specific phosphoinositide 3-kinase inhibitors from an arylmorpholine scaffold. *Bioorg. Med. Chem. Lett.* **2004**, *12*, 4749–4759. [CrossRef] [PubMed]

76. Durant, S.; Karran, P. Vanillins—A novel family of DNA-PK inhibitors. *Nucleic Acids Res.* **2003**, *31*, 5501–5512. [CrossRef] [PubMed]

77. Ismail, I.H.; Marternsson, S.; Moshinsky, D.; Rice, A.; Tang, C.; Howlett, A.; McMahon, G.; Hammarste, O. SU11752 inhibits the DNA-dependent protein kinase and DNA double-strand break repair resulting in ionizing radiation sensitization. *Oncogene* **2004**, *23*, 873–882. [CrossRef]

78. Fan, Q.W.; Knight, Z.A.; Goldenberg, D.D.; Yu, W.; Mostov, K.E.; Stokoe, D.; Shokat, K.M.; Weiss, W.A. A dual PI3 kinase/mTOR inhibitor reveals emergent efficacy in glioma. *Cancer Cell* **2006**, *9*, 341–349. [CrossRef]

79. Kong, D.; Yaguchi, S.; Yamori, T. Effect of ZSTK474, a novel phosphatidylinositol 3-kinase inhibitor, on DNA-dependent protein kinase. *Biol. Pharm. Bull.* **2009**, *32*, 297–300. [CrossRef]

80. Toledo, L.I.; Murga, M.; Zur, R.; Soria, R.; Rodriguez, A.; Martinez, S.; Oyarzabal, J.; Pastor, J.; Bischoff, J.R.; Fernandez-Capetillo, O. A cell-based screen identifies ATR inhibitors with synthetic lethal properties for cancer-associated mutations. *Nat. Struct. Mol. Biol.* **2011**, *18*, 721–727. [CrossRef]

81. Smith, M.C.; Mader, M.M.; Cook, J.A.; Iversen, P.; Ajamie, R.; Perkins, E.; Bloem, L.; Yip, Y.Y.; Barda, D.A.; Waid, P.P.; et al. Characterization of LY3023414, a Novel PI3K/mTOR Dual Inhibitor Eliciting Transient Target Modulation to Impede Tumor Growth. *Mol. Cancer Ther.* **2016**, *15*, 2344–2356. [CrossRef]

82. Mortensen, D.S.; Perrin-Ninkovic, S.M.; Shevlin, G.; Elsner, J.; Zhao, J.; Whitefield, B.; Tehrani, L.; Sapienza, J.; Riggs, J.R.; Parnes, J.S.; et al. Optimization of a Series of Triazole Containing Mammalian Target of Rapamycin (mTOR) Kinase Inhibitors and the Discovery of CC-115. *J. Med. Chem.* **2015**, *58*, 5599–5608. [CrossRef]

83. Sun, Q.; Guo, Y.; Liu, X.; Czauderna, F.; Carr, M.I.; Zenke, F.T.; Blaukat, A.; Vassilev, L.T. Therapeutic Implications of p53 Status on Cancer Cell Fate Following Exposure to Ionizing Radiation and the DNA-PK Inhibitor M3814. *Mol. Cancer Res.* **2019**, *17*, 2457–2468. [CrossRef]

84. Sarkaria, J.N.; Tibbetts, R.S.; Busby, E.C.; Kennedy, A.P.; Hill, D.E.; Abraham, R.T. Inhibition of phosphoinositide 3-kinase related kinases by the radiosensitizing agent wortmannin. *Cancer Res.* **1998**, *58*, 4375–4382.

85. Rosenzweig, K.E.; Youmell, M.B.; Palayoor, S.T.; Price, B.D. Radiosensitization of human tumor cells by the phosphatidylinositol3-kinase inhibitors wortmannin and LY294002 correlates with inhibition of DNA-dependent protein kinase and prolonged G2-M delay. *Clin. Cancer Res.* **1997**, *3*, 1149–1156.

86. Okayasu, R.; Suetomi, K.; Ullrich, R.L. Wortmannin inhibits repair of DNA double-strand breaks in irradiated normal human cells. *Radiat. Res.* **1998**, *149*, 440–445. [CrossRef]

87. Vlahos, C.J.; Matter, W.F.; Hui, K.Y.; Brown, R.F. A specific inhibitor of phosphatidylinositol 3-kinase, 2-(4-morpholinyl)-8-phenyl-4H-1-benzopyran-4-one (LY294002). *J. Biol. Chem.* **1994**, *269*, 5241–5248. [CrossRef]

88. Hollick, J.J.; Golding, B.T.; Hardcastle, I.R.; Martin, N.; Richardson, C.; Rigoreau, L.J.; Smith, G.C.; Griffin, R.J. 2,6-disubstituted pyran-4-one and thiopyran-4-one inhibitors of DNA-Dependent protein kinase (DNA-PK). *Bioorg. Med. Chem. Lett.* **2003**, *13*, 3083–3086. [CrossRef]

89. Willmore, E.; de Caux, S.; Sunter, N.J.; Tilby, M.J.; Jackson, G.H.; Austin, C.A.; Durkacz, B.W. A novel DNA-dependent protein kinase inhibitor, NU7026, potentiates the cytotoxicity of topoisomerase II poisons used in the treatment of leukemia. *Blood* **2004**, *103*, 4659–4665. [CrossRef]

90. Nutley, B.P.; Smith, N.F.; Hayes, A.; Kelland, L.R.; Brunton, L.; Golding, B.T.; Smith, G.C.; Martin, N.M.; Workman, P.; Raynaud, F.I. Preclinical pharmacokinetics and metabolism of a novel prototype DNA-PK inhibitor NU7026. *Br. J. Cancer* **2005**, *93*, 1011–1018. [CrossRef]

91. Zhen, Y.F.; Li, S.T.; Zhu, Y.R.; Wang, X.D.; Zhou, X.Z.; Zhu, L.Q. Identification of DNA-PKcs as a primary resistance factor of salinomycin in osteosarcoma cells. *Oncotarget* **2016**, *7*, 79417–79427. [CrossRef]

92. Cheng, L.; Liu, Y.Y.; Lu, P.H.; Peng, Y.; Yuan, Q.; Gu, X.S.; Jin, Y.; Chen, M.B.; Bai, X.M. Identification of DNA-PKcs as a primary resistance factor of TIC10 in hepatocellular carcinoma cells. *Oncotarget* **2017**, *8*, 28385–28394. [CrossRef]

93. Yang, L.; Yang, X.; Tang, Y.; Zhang, D.; Zhu, L.; Wang, S.; Wang, B.; Ma, T. Inhibition of DNA-PK activity sensitizes A549 cells to X-ray irradiation by inducing the ATM-dependent DNA damage response. *Mol. Med. Rep.* **2018**, *17*, 7545–7552. [CrossRef]

94. Hardcastle, I.R.; Cockcroft, X.; Curtin, N.J.; El-Murr, M.D.; Leahy, J.J.J.; Stockley, M.; Golding, B.T.; Rigoreau, L.; Richardson, C.; Smith, G.C.M.; et al. Discovery of potent chromen-4-one inhibitors of the DNA-dependent protein kinase (DNA-PK) using a small-molecule library approach. *J. Med. Chem.* **2005**, *48*, 7829–7846. [CrossRef]

95. Zhao, Y.; Thomas, H.D.; Matey, M.A.; Cowell, I.G.; Rihardson, C.J.; Griffin, R.J.; Calvert, A.H.; Newell, D.R.; Smith, G.C.M.; Curtin, N.J. Preclinical evaluation of a potent novel DNA-dependent protein kinase inhibitor NU7441. *Cancer Res.* **2006**, *66*, 5354–5362. [CrossRef]

96. Yu, L.; Shang, Z.F.; Hsu, F.M.; Zhang, Z.; Tumati, V.; Lin, Y.F.; Chen, B.P.; Saha, D. NSCLC cells demonstrate differential mode of cell death in response to the combined treatment of radiation and a DNA-PKcs inhibitor. *Oncotarget* **2015**, *6*, 3848–3860. [CrossRef] [PubMed]

97. Munck, J.M.; Batey, M.A.; Zhao, Y.; Jenkins, H.; Richardson, C.J.; Cano, C.; Tavecchio, M.; Barbeau, J.; Bardos, J.; Cornell, L.; et al. Chemosensitization of cancer cells by KU-0060648, a dual inhibitor of DNA-PK and PI-3K. *Mol. Cancer Ther.* **2012**, *11*, 1789–1798. [CrossRef] [PubMed]

98. Chen, M.B.; Zhou, Z.T.; Yang, L.; Wei, M.X.; Tang, M.; Ruan, T.Y.; Xu, J.Y.; Zhou, X.Z.; Chen, G.; Lu, P.H. KU-0060648 inhibits hepatocellular carcinoma cells through DNA-PKcs-dependent and DNA-PKcs-independent mechanisms. *Oncotarget* **2016**, *7*, 17047–17059. [CrossRef] [PubMed]

99. Lan, T.; Zhao, Z.; Qu, Y.; Zhang, M.; Wang, H.; Zhang, Z.; Zhou, W.; Fan, X.; Yu, C.; Zhan, Q.; et al. Targeting hyperactivated DNA-PKcs by KU0060648 inhibits glioma progression and enhances temozolomide therapy via suppression of AKT signaling. *Oncotarget* **2016**, *7*, 55555–55571. [CrossRef] [PubMed]

100. Chao, O.S.; Goodman, O.B., Jr. DNA-PKc inhibition overcomes taxane resistance by promoting taxane-induced DNA damage in prostate cancer cells. *Prostate* **2021**, *81*, 1032–1048. [CrossRef] [PubMed]

101. Hickson, I.; Zhao, Y.; Richardoson, C.J.; Green, S.J.; Martin, N.M.B.; Orr, A.I.; Reaper, P.M.; Jackson, S.P.; Curtin, N.J.; Smith, G.C.M. Identification and characterization of a novel and specific inhibitor of the ataxia-telangiectasia mutated kinase ATM. *Cancer Res.* **2004**, *64*, 9152–9159. [CrossRef] [PubMed]

102. Golding, S.E.; Rosenberg, E.; Valerie, N.; Hussaini, I.; Frigerio, M.; Cockcroft, X.F.; Chong, W.Y.; Hummersone, M.; Rigoreau, L.; Menear, K.A.; et al. Improved ATM kinase inhibitor KU-60019 radiosensitizes glioma cells, compromises insulin, AKT and ERK prosurvival signaling, and inhibits migration and invasion. *Mol. Cancer Ther.* **2009**, *8*, 2894–2902. [CrossRef]

103. Sturgeon, C.M.; Knight, Z.A.; Shokat, K.M.; Roberge, M. Effect of combined DNA repair inhibition and G2 checkpoint inhibition on cell cycle progression after DNA damage. *Mol. Cancer Ther.* **2006**, *5*, 885–892. [CrossRef]

104. Westhoff, M.A.; Kandenwein, J.A.; Karl, S.; Vellanki, S.H.; Braun, V.; Eramo, A.; Antoniadis, G.; Debatin, K.M.; Fulda, S. The pyridinylfuranopyrimidine inhibitor, PI-103, chemosensitizes glioblastoma cells for apoptosis by inhibiting DNA repair. *Oncogene* **2009**, *28*, 3586–3596. [CrossRef]

105. Mukherjee, B.; Tomimatsu, N.; Amancherla, K.; Camacho, C.V.; Pichamoorthy, N.; Burma, S. The dual PI3K/mTOR inhibitor NVP-BEZ235 is a potent inhibitor of ATM- and DNAPKcs-mediated DNA damage responses. *Neoplasia* **2012**, *14*, 34–43. [CrossRef]

106. Gil del Alcazar, C.R.; Hardebeck, M.C.; Mukherjee, B.; Tomimatsu, N.; Gao, X.; Yan, J.; Xie, X.J.; Bachoo, R.; Li, L.; Habib, A.A.; et al. Inhibition of DNA double-strand break repair by the dual PI3K/mTOR inhibitor NVP-BEZ235 as a strategy for radiosensitization of glioblastoma. *Clin. Cancer Res.* **2014**, *20*, 1235–1248. [CrossRef]

107. Bürkel, F.; Jost, T.; Hecht, M.; Heinzerling, L.; Fietkau, R.; Distel, L. Dual mTOR/DNA-PK Inhibitor CC-115 Induces Cell Death in Melanoma Cells and Has Radiosensitizing Potential. *Int. J. Mol. Sci.* **2020**, *21*, 9321. [CrossRef]

108. Timme, C.R.; Rath, B.H.; O'Neill, J.W.; Camphausen, K.; Tofilon, P.J. The DNA-PK Inhibitor VX-984 Enhances the Radiosensitivity of Glioblastoma Cells Grown In Vitro and as Orthotopic Xenografts. *Mol. Cancer Ther.* **2018**, *17*, 1207–1216. [CrossRef]

109. Carr, M.I.; Zimmermann, A.; Chiu, L.Y.; Zenke, F.T.; Blaukat, A.; Vassilev, L.T. DNA-PK Inhibitor, M3814, as a New Combination Partner of Mylotarg in the Treatment of Acute Myeloid Leukemia. *Front Oncol.* **2020**, *10*, 127. [CrossRef]

110. Zenke, F.T.; Zimmermann, A.; Sirrenberg, C.; Dahmen, H.; Kirkin, V.; Pehl, U.; Grombacher, T.; Wilm, C.; Fuchss, T.; Amendt, C.; et al. Pharmacologic Inhibitor of DNA-PK, M3814, Potentiates Radiotherapy and Regresses Human Tumors in Mouse Models. *Mol. Cancer Ther.* **2020**, *19*, 1091–1101. [CrossRef]

111. Haines, E.; Nishida, Y.; Carr, M.I.; Montoya, R.H.; Ostermann, L.B.; Zhang, W.; Zenke, F.T.; Blaukat, A.; Andreeff, M.; Vassilev, L.T. DNA-PK inhibitor peposertib enhances p53-dependent cytotoxicity of DNA double-strand break inducing therapy in acute leukemia. *Sci. Rep.* **2021**, *11*, 12148. [CrossRef]

112. Smithson, M.; Irwin, R.K.; Williams, G.; McLeod, M.C.; Choi, E.K.; Ganguly, A.; Pepple, A.; Cho, C.S.; Willey, C.D.; Leopold, J.; et al. Inhibition of DNA-PK may improve response to neoadjuvant chemoradiotherapy in rectal cancer. *Neoplasia* **2022**, *25*, 53–61. [CrossRef] [PubMed]

113. Wang, M.; Chen, S.; Wei, Y.; Wei, X. DNA-PK inhibition by M3814 enhances chemosensitivity in non-small cell lung cancer. *Acta. Pharm. Sin. B* **2021**, *11*, 3935–3949. [CrossRef] [PubMed]

114. Wise, H.C.; Iyer, G.V.; Moore, K.; Temkin, S.M.; Gordon, S.; Aghajanian, C.; Grisham, R.N. Activity of M3814, an Oral DNA-PK Inhibitor, In Combination with Topoisomerase II Inhibitors in Ovarian Cancer Models. *Sci. Rep.* **2019**, *9*, 18882. [CrossRef] [PubMed]

115. Gordhandas, S.B.; Manning-Geist, B.; Henson, C.; Iyer, G.; Gardner, G.J.; Sonoda, Y.; Moore, K.N.; Aghajanian, C.; Chui, M.H.; Grisham, R.N. Pre-clinical activity of the oral DNA-PK inhibitor, peposertib (M3814), combined with radiation in xenograft models of cervical cancer. *Sci. Rep.* **2022**, *12*, 974. [CrossRef]

116. Carr, M.I.; Chiu, L.Y.; Guo, Y.; Xu, C.; Lazorchak, A.S.; Yu, H.; Qin, G.; Qi, J.; Marelli, B.; Lan, Y.; et al. DNA-PK Inhibitor Peposertib Amplifies Radiation-Induced Inflammatory Micronucleation and Enhances TGFbeta/PD-L1 Targeted Cancer Immunotherapy. *Mol. Cancer Res.* 2022; *online ahead of print*. [CrossRef]

117. Nakamura, K.; Karmokar, A.; Farrington, P.M.; James, N.H.; Ramos-Montoya, A.; Bickerton, S.J.; Hughes, G.D.; Illidge, T.M.; Cadogan, E.B.; Davies, B.R.; et al. Inhibition of DNA-PK with AZD7648 Sensitizes Tumor Cells to Radiotherapy and Induces Type I IFN-Dependent Durable Tumor Control. *Clin. Cancer Res.* **2021**, *27*, 4353–4366. [CrossRef]

118. Hong, C.R.; Buckley, C.D.; Wong, W.W.; Anekal, P.V.; Dickson, B.D.; Bogle, G.; Hicks, K.O.; Hay, M.P.; Wilson, W.R. Radiosensitisation of SCCVII tumours and normal tissues in mice by the DNA-dependent protein kinase inhibitor AZD7648. *Radiother. Oncol.* **2022**, *166*, 162–170. [CrossRef]

119. Anastasia, A.; Dellavedova, G.; Ramos-Montoya, A.; James, N.H.; Chiorino, G.; Russo, M.; Baakza, H.; Wilson, J.; Ghilardi, C.; Cadogan, E.B.; et al. The DNA-PK inhibitor AZD7648 sensitizes patient derived ovarian cancer xenografts to pegylated liposomal doxorubicin and olaparib preventing abdominal metastases. *Mol. Cancer Ther.* 2022; *online ahead of print*. [CrossRef]

120. Shinohara, E.T.; Geng, L.; Tan, J.; Chen, H.; Shir, Y.; Edwards, E.; Halbrook, J.; Kesicki, E.A.; Kashishian, A.; Hallahan, D.E. DNA-dependent protein kinase is a molecular target for the development of noncytotoxic radiation-sensitizing drugs. *Cancer Res.* **2005**, *65*, 4987–4992. [CrossRef]

121. Wong, W.W.; Jackson, R.K.; Liew, L.P.; Dickson, B.D.; Cheng, G.J.; Lipert, B.; Gu, Y.; Hunter, F.W.; Wilson, W.R.; Hay, M.P. Hypoxia-selective radiosensitisation by SN38023, a bioreductive prodrug of DNA-dependent protein kinase inhibitor IC87361. *Biochem. Pharmacol.* **2019**, *169*, 113641. [CrossRef]

122. Zheng, H.; Chen, Z.W.; Wang, L.; Wang, S.Y.; Yan, Y.Q.; Wu, K.; Xu, Q.Z.; Zhang, S.M.; Zhou, P.K. Radioprotection of 4-hydroxy-3,5-dimethoxybenzaldehyde (VND3207) in culture cells is associated with minimizing DNA damage and activating Akt. *Eur. J. Pharm. Sci.* **2008**, *33*, 52–59. [CrossRef]

123. Li, M.; Lang, Y.; Gu, M.M.; Shi, J.; Chen, B.P.C.; Yu, L.; Zhou, P.K.; Shang, Z.F. Vanillin derivative VND3207 activates DNA-PKcs conferring protection against radiation-induced intestinal epithelial cells injury in vitro and in vivo. *Toxicol. Appl. Pharmacol.* **2020**, *387*, 114855. [CrossRef]

124. Hayakawa, M.; Kaizawa, H.; Moritomo, H.; Koizumi, T.; Ohishi, T.; Yamano, M.; Okada, M.; Ohta, M.; Tsukamoto, S.; Raynaud, F.I.; et al. Synthesis and biological evaluation of pyrido [3',2':4,5]furo [3,2-d]pyrimidine derivatives as novel PI3 kinase p110alpha inhibitors. *Bioorg. Med. Chem. Lett.* **2007**, *17*, 2438–2442. [CrossRef]

125. Raynaud, F.I.; Eccles, S.; Clarke, P.A.; Hayes, A.; Nutley, B.; Alix, S.; Henley, A.; Di-Stefano, F.; Ahmad, Z.; Guillard, S.; et al. Pharmacologic characterization of a potent inhibitor of class I phosphatidylinositide 3-kinases. *Cancer Res.* **2007**, *67*, 5840–5850. [CrossRef]

126. Zhu, H.; Mishra, R.; Yuan, L.; Salam, S.F.A.; Liu, J.; Gray, G.; Sterling, A.D.; Wunderlich, M.; Landero-Figueroa, J.; Garrett, J.T.; et al. Oxidative cyclization-induced activation of a phosphoinositide 3-kinase inhibitor for enhanced selectivity of cancer chemotherapeutics. *Chem. Med. Chem.* **2019**, *14*, 1933–1939. [CrossRef]

127. Mishra, R.; Yuan, L.; Patel, H.; Karve, A.S.; Zhu, H.; White, A.; Alanazi, S.; Desai, P.; Merino, E.J.; Garrett, J.T. Phosphoinositide 3-Kinase (PI3K) Reactive Oxygen Species (ROS)-Activated Prodrug in Combination with Anthracycline Impairs PI3K Signaling, Increases DNA Damage Response and Reduces Breast Cancer Cell Growth. *Int. J. Mol. Sci.* **2021**, *22*, 2088. [CrossRef]

128. Maira, S.M.; Stauffer, F.; Brueggen, J.; Furet, P.; Schnell, C.; Fritsch, C.; Brachmann, S.; Chene, P.; De Pover, A.; Schoemaker, K.; et al. Identification and characterization of NVP-BEZ235, a new orally available dual phosphatidylinositol 3-kinase/mammalian target of rapamycin inhibitor with potent in vivo antitumor activity. *Mol. Cancer Ther.* **2008**, *7*, 1851–1863. [CrossRef]

129. Seront, E.; Rottey, S.; Filleul, B.; Glorieux, P.; Goeminne, J.C.; Verschaeve, V.; Vandenbulcke, J.M.; Sautois, B.; Boegner, P.; Gillain, A.; et al. Phase II study of dual phosphoinositol-3-kinase (PI3K) and mammalian target of rapamycin (mTOR) inhibitor BEZ235 in patients with locally advanced or metastatic transitional cell carcinoma. *BJU Int.* **2016**, *118*, 408–415. [CrossRef]

130. Fazio, N.; Buzzoni, R.; Baudin, E.; Antonuzzo, L.; Hubner, R.A.; Lahner, H.; de Herder, W.W.; Raderer, M.; Teulé, A.; Capdevila, J.; et al. A Phase II Study of BEZ235 in Patients with Everolimus-resistant, Advanced Pancreatic Neuroendocrine Tumours. *Anticancer Res.* **2016**, *36*, 713–719.

131. Salazar, R.; Garcia-Carbonero, R.; Libutti, S.K.; Hendifar, A.E.; Custodio, A.; Guimbaud, R.; Lombard-Bohas, C.; Ricci, S.; Klümpen, H.J.; Capdevila, J.; et al. Phase II Study of BEZ235 versus Everolimus in Patients with Mammalian Target of Rapamycin Inhibitor-Naïve Advanced Pancreatic Neuroendocrine Tumors. *Oncologist* **2018**, *23*, 766–790. [CrossRef]

132. Bendell, J.C.; Varghese, A.M.; Hyman, D.M.; Bauer, T.M.; Pant, S.; Callies, S.; Lin, J.; Martinez, R.; Wickremsinhe, E.; Fink, A.; et al. A First-in-Human Phase 1 Study of LY3023414, an Oral PI3K/mTOR Dual Inhibitor, in Patients with Advanced Cancer. *Clin. Cancer Res.* **2018**, *24*, 3253–3262. [CrossRef]

133. Kondo, S.; Tajimi, M.; Funai, T.; Inoue, K.; Asou, H.; Ranka, V.K.; Wacheck, V.; Doi, T. Phase 1 dose-escalation study of a novel oral PI3K/mTOR dual inhibitor, LY3023414, in patients with cancer. *Investig. New Drugs* **2020**, *38*, 1836–1845. [CrossRef]

134. Zauderer, M.G.; Alley, E.W.; Bendell, J.; Capelletto, E.; Bauer, T.M.; Callies, S.; Szpurka, A.M.; Kang, S.; Willard, M.D.; Wacheck, V.; et al. Phase 1 cohort expansion study of LY3023414, a dual PI3K/mTOR inhibitor, in patients with advanced mesothelioma. *Investig. New Drugs* **2021**, *39*, 1081–1088. [CrossRef]

135. Rubinstein, M.M.; Hyman, D.M.; Caird, I.; Won, H.; Soldan, K.; Seier, K.; Iasonos, A.; Tew, W.P.; O'Cearbhaill, R.E.; Grisham, R.N.; et al. Phase 2 study of LY3023414 in patients with advanced endometrial cancer harboring activating mutations in the PI3K pathway. *Cancer* **2020**, *126*, 1274–1282. [CrossRef]

136. Azaro, A.; Massard, C.; Tap, W.D.; Cassier, P.A.; Merchan, J.; Italiano, A.; Anderson, B.; Yuen, E.; Yu, D.; Oakley, G., 3rd; et al. A phase 1b study of the Notch inhibitor crenigacestat (LY3039478) in combination with other anticancer target agents (taladegib, LY3023414, or abemaciclib) in patients with advanced or metastatic solid tumors. *Investig. New Drugs* **2021**, *39*, 1089–1098. [CrossRef]

137. Tsuji, T.; Sapinoso, L.M.; Tran, T.; Gaffney, B.; Wong, L.; Sankar, S.; Raymon, H.K.; Mortensen, D.S.; Xu, S. CC-115, a dual inhibitor of mTOR kinase and DNA-PK, blocks DNA damage repair pathways and selectively inhibits ATM-deficient cell growth in vitro. *Oncotarget* **2017**, *8*, 74688–74702. [CrossRef]

138. Zheng, B.; Sun, X.; Chen, X.F.; Chen, Z.; Zhu, W.L.; Zhu, H.; Gu, D.H. Dual inhibition of DNA-PKcs and mTOR by CC-115 potently inhibits human renal cell carcinoma cell growth. *Aging (Albany N. Y.)* **2020**, *12*, 20445–20456. [CrossRef]

139. Thijssen, R.; Ter Burg, J.; Garrick, B.; van Bochove, G.G.; Brown, J.R.; Fernandes, S.M.; Rodríguez, M.S.; Michot, J.M.; Hallek, M.; Eichhorst, B.; et al. Dual TORK/DNA-PK inhibition blocks critical signaling pathways in chronic lymphocytic leukemia. *Blood* **2016**, *128*, 574–583. [CrossRef]

140. Munster, P.; Mita, M.; Mahipal, A.; Nemunaitis, J.; Massard, C.; Mikkelsen, T.; Cruz, C.; Paz-Ares, L.; Hidalgo, M.; Rathkopf, D.; et al. First-In-Human Phase I Study Of A Dual mTOR Kinase And DNA-PK Inhibitor (CC-115) In Advanced Malignancy. *Cancer Manag. Res.* **2019**, *11*, 10463–10476. [CrossRef]

141. Khan, A.J.; Misenko, S.M.; Thandoni, A.; Schiff, D.; Jhawar, S.R.; Bunting, S.F.; Haffty, B.G. VX-984 is a selective inhibitor of non-homologous end joining, with possible preferential activity in transformed cells. *Oncotarget* **2018**, *9*, 25833–25841. [CrossRef]

142. Wu, Z.X.; Peng, Z.; Yang, Y.; Wang, J.Q.; Teng, Q.X.; Lei, Z.N.; Fu, Y.G.; Patel, K.; Liu, L.; Lin, L.; et al. M3814, a DNA-PK Inhibitor, Modulates ABCG2-Mediated Multidrug Resistance in Lung Cancer Cells. *Front. Oncol.* **2020**, *10*, 674. [CrossRef]

143. Van Bussel, M.T.J.; Awada, A.; de Jonge, M.J.A.; Mau-Sørensen, M.; Nielsen, D.; Schöffski, P.; Verheul, H.M.W.; Sarholz, B.; Berghoff, K.; El Bawab, S.; et al. A first-in-man phase 1 study of the DNA-dependent protein kinase inhibitor peposertib (formerly M3814) in patients with advanced solid tumours. *Br. J. Cancer* **2021**, *124*, 728–735. [CrossRef]

144. Goldberg, F.W.; Finlay, M.R.V.; Ting, A.K.T.; Beattie, D.; Lamont, G.M.; Fallan, C.; Wrigley, G.L.; Schimpl, M.; Howard, M.R.; Williamson, B.; et al. The Discovery of 7-Methyl-2-[(7-methyl [1,2,4]triazolo [1,5-a]pyridin-6-yl)amino]-9-(tetrahydro-2H-pyran-4-yl)-7,9-dihydro-8H-purin-8-one (AZD7648), a Potent and Selective DNA-Dependent Protein Kinase (DNA-PK) Inhibitor. *J. Med. Chem.* **2020**, *63*, 3461–3471. [CrossRef] [PubMed]

145. Patel, A.G.; Sarkaria, J.N.; Kaufmann, S.H. Nonhomologous end joining drives poly(ADP-ribose) polymerase (PARP) inhibitor lethality in homologous recombination-deficient cells. *Proc. Natl. Acad. Sci. USA* **2011**, *108*, 3406–3411. [CrossRef] [PubMed]

146. Williamson, C.T.; Kubota, E.; Hamill, J.D.; Klimowicz, A.; Ye, R.; Muzik, H.; Dean, M.; Tu, L.; Gilley, D.; Magliocco, A.M.; et al. Enhanced cytotoxicity of PARP inhibition in mantle cell lymphoma harbouring mutations in both ATM and p53. *EMBO Mol. Med.* **2012**, *4*, 515–527. [CrossRef] [PubMed]

147. Van Os, N.J.; Roeleveld, N.; Weemaes, C.M.; Jongmans, M.C.; Janssens, G.O.; Taylor, A.M.; Hoogerbrugge, N.; Willemsen, M.A. Health risks for ataxia-telangiectasia mutated heterozygotes: A systematic review, meta-analysis and evidence-based guideline. *Clin. Genet.* **2016**, *90*, 105–117. [CrossRef] [PubMed]

148. Jerzak, K.J.; Mancuso, T.; Eisen, A. Ataxia-telangiectasia gene (ATM) mutation heterozygosity in breast cancer: A narrative review. *Curr. Oncol.* **2018**, *25*, 176–180. [CrossRef] [PubMed]